Bachelor Graduation Project Thesis

Battery Free Jogger Light
Lighting & Casing

Written by:
Jory Edelman
Bart van Nobelen

Delft University of Technology

TU Delft Delft University of Technology

Challenge the future

Bachelor Graduation Project

Battery Free Jogger Light
Lighting & Casing

Jory Edelman
Bart van Nobelen

Supervisors:
Dr. Massimo Mastrangeli
Dr. Virgilio Valente

A thesis presented for the degree of
BSc Electrical Engineering

Faculty of Electrical Engineering, Mathematics & Computer Science
(EEMCS)
Delft University of Technology

Abstract

This document describes the design process and implementation of the lighting and casing of a battery free jogger light. This light is meant to increase the safety of joggers in dark environments. The most effective way of increasing the jogger's conspicuity will be researched by considering different light sources and driver circuits to efficiently power the light source in a blinking manner. A casing will be designed to encapsulate the components. Light emitting diodes were chosen as a light source due to their energy efficiency, colour optimisation and small size. Two LEDs are part of a rectifier, while three other LEDs are powered by a driver circuit that uses a clocked decade counter 4017 IC that receives its clock signal from a NAND based oscillator circuit. The casing is designed with 3D modelling software and a prototype is 3D printed. The intended light intensity was not reached, but the brightness in dark environments was deemed suitable for the project's goals. The casing has bigger dimensions than intended; however these can be optimised for mass production.

Preface

This thesis is written as part of the Bachelor Graduation Project of Electrical Engineering at the Delft University of Technology. The project Battery Free Jogger Light was proposed by Dr. John Schmitz and Dr. Massimo Mastrangeli as they are both joggers and were very interested in a solution for a problem they had: jogging lights running out of batteries. So we took on this project and worked for two hard but enjoyable months towards a result we can be proud of. We made a jogger light which will never run out of batteries and will always be ready to go, it will even keep blinking when you're standing still.

We would like to sincerely thank our supervisor Dr. Massimo Mastrangeli and co-supervisor Dr. Virgilio Valente for their excellent guidance, interest in the project and answers to all of our questions. Furthermore we would like to thank Mr. Martin Schumacher for his great spirit in the Tellegen Hall and for ordering all the components we needed for our project. Finally we would like to thank Boyd Riemens, Koen Mesman, Jelle Klein and Jhorie Slot, which were our colleagues in this project. Without them the achieved results wouldn't be possible and they made for a very productive and enjoyable collaboration.

Jory Edelman & Bart van Nobelen
Delft, June 2019

Contents

Chapter 1

Introduction

According to a report of the World Health Organization, the occurrence of road traffic accidents worldwide increases and results in about 1,200,000 deaths and more than 5,000,000 injured people every year. The report predicts that road traffic accidents will, in 2020, be the third largest killer of human life. However, distinctive road signs designed with reflective materials and well illuminated road users could decrease the accident rate by 30% to 40%. This is due to the rate of traffic accidents, associated with the visibility of road users and road signs, is close to 70%, as indicated by statistics which are provided by a foreign investigating authority [1].

One of the most vulnerable road users are the joggers. It is therefore of importance that joggers can run safely in the dark, as not everyone is able to go jogging during the day. Back in the days people used to go jogging without any lights, and thus were poorly visible in the dark, which resulted in a high risk of accidents. Nowadays there is an increasing awareness of the importance of personal safety in traffic, causing most people to use some sort of visibility aid when they go jogging in the dark. The best option when it comes to increased conspicuity of the jogger, is using a light source [2]. It is therefore important that attention drawing, comfortable, and durable jogging lights are available for joggers.

Loads of different jogger orientated lighting products are currently available. However, most of them power their light source using batteries. These products often feature batteries that are not rechargeable and it is often more convenient to replace the whole product rather than the batteries. An exception, the Million Mile Light [3], powers its light source by harvesting energy from human motion instead. This significantly increases the lifetime of the product and removes the inconvenience of untimely dying batteries. The disadvantages of the Million Mile Light are the emission of light being limited to 180°, for one product, and the lack of light emission when the jogger stops moving.

Improvements can be made on the concept of the the Million Mile Light by powering the light source for a certain time period after the jogger has stopped moving, while also increasing the angle that the light source covers. Different ways of harvesting energy can also be considered, as to find the most efficient way of harvesting power. Some kind of energy storage will be necessary to prolong the light emission after movement has stopped. The light should flash, as this ensures better visibility in the dark according to studies [4].

The goal of this project is to design such a product, for which the task can be defined as: Design a battery free light which joggers can wear, that emits a flashing light while jogging and a short time period thereafter.

The environmental footprint of the product should be an improvement over the conventional jogger lights. Since no batteries will be used in the product, the production is more environmentally friendly and the durability is increased, which also improves its environmental footprint. As it is a low power light, the impact on light pollution will also be minimal.

The project is split up in three parts, the energy harvester, the energy conversion and storage and the lighting and the casing of the product. This thesis will focus on the lighting and the

design of the casing. For lighting different kinds of light sources and their specifications will be discussed as well as the placement of the product on the body and the advantage of flashing over continuous lights. Different methods for powering the light source, in a flashing manner, will be analysed. The product needs a casing for the components to be assembled in. The different parts of the casing and materials that can be used for it, are compared. Lastly, the design is implemented and the prototype will be produced.

Chapter 2

Programme of Requirements

The goal of this project is to design a battery free jogger light. In order to comply to the standards set by the proposer of the project a list of requirements for the final design were set up. In the program of requirements a difference is made between mandatory and trade-off requirements. The requirements which apply to the lighting and casing are the ones which are shown in bold.

Mandatory requirements are:

- Must not have a battery
- **Must have a flashing light**
- **The frequency of the flashing must be independent of the jogger's movement**
- Must function in every moment of the day
- **Must have a light intensity of at least 4 candela (cd)**
- **Must be wearable: Max. 250 g (incl. casing)**
- **Must not obstruct the running movement**
- **Must not be harmful for the jogger**
- Must be able to store energy for 30 seconds of lighting, when fully charged
- Must be fully charged within 2 minutes of jogging
- **Casing must be water-resistant (IP54)**
- **Angle of lighting must be at least 180°**
- Must have a life time of at least 3600 jogging hours (2 hours per day, for 5 years)
- **Max. depth dimension is 2.5 cm**
- **Max. €50 material costs for the final prototype**

Trade-off requirements are:

- **Maximise light intensity (cd)**
- **Maximise angle of visibility**
- Maximise harvested power
- **Maximise flashing duration when standing still**
- **Maximise durability**
- **Minimise weight**
- **Minimise volume**
- **Minimise production costs**
- Minimise charging time

The product must have a flashing light and an angle of lighting of at least 180°, as this increases the conspicuity of the user. The light intensity of four candela comes from the minimal allowed light intensity of cyclists in the United Kingdom. The weight is limited to 250 grams as to ensure comfort while wearing the product. Similarly, the depth is limited to 2.5 cm as to prevent the product from sticking out too much. As the product is used outdoors, water resistance is a necessity for dealing with rain. The material costs of the prototype are limited to €50, as to prevent initially high production costs of the product.

Chapter 3

Design Process

3.1 Product location on the body

The location on the body at which the product will be worn, is an important decision that affects the design of the product's casing, the visibility of the jogger, the comfort of wearing the product and the power harvested by the product. Two options are considered, these should maximise visibility while maintaining the comfort of the jogger. These are the waist and the upper arm. The product is expected to minimally impact the natural movement of the runner when located at these positions. This expectation is mainly based on jogger accessories that are currently available, which are to be worn at these body locations. The energy harvesting group has indicated that waist is the most suitable location for producing sufficient power. Visibility wise, the preference goes out to wearing the product on the upper arm, as the location is higher up the body, which makes it harder for objects to obstruct the visibility of the product to other road users. Additionally, wearing the product on a moving body part stimulates the recognition of human motion, making it easier for the jogger to be detected and recognised by others [5].

3.2 Background information

Before considering what type of lighting and corresponding specifications to choose, it is important to realise how light acts and is detected by the human eye in the setting which the product is used in. This section will first describe the setting that the product is assumed and intended to be used in. This is followed by background information on the perception of light by the human eye and how this impacts lighting specifications. Lastly a part on the advantage of implementing a blinking light source for our product is covered.

3.2.1 Setting

Due to the product's nature it is safe to assume a night-time setting or a setting with reduced visibility compared to a clear day. The environmental lights are assumed, out of empirical consideration, to be majorly dominated by non-flashing light sources; barring any exceptions. The jogger will primarily be approached by other traffic from the front and the back. Only at junctions should the jogger ever be approached from his/her side.

3.2.2 The perception of light

The human eye contains two classes of photoreceptive cells, which are specialised for the capture of light. These are the so-called rods and cones, see Figure A.1b, which are responsible for monochromatic vision at dim light and trichromatic vision in daylight respectively [6]. Three different vision regions that are associated with the activity of these cells, are the scotopic, photopic and mesopic regions. These regions correspond to the exclusive activity of the rods, the exclusive activity of the cones and the activity of both rods and cones respectively. Similarly,

the associated luminous range of these regions are the minimum visible stimulus up to approximately $0.001cd/m^2$, $10cd/m^2$ up to the highest visible stimulus and $0.001cd/m^2$ up to $10cd/m^2$ respectively [7].
The luminosity in night traffic settings, that the product is considered to be used in, is in the mesopic region [8]. Important to note is that the luminous efficacy, the amount of lumen emitted per unit of power supplied, is calculated considering the photopic region rather than the mesopic region. Therefore the ratio of scotopic-to-photopic luminous flux, the scotopic/photopic (S/P) ratio, is an import parameter that relates luminous quantities to the mesopic region [7].

3.2.3 Blinking light sources

In the early 19th century it was observed that using a blinking light for lighthouses produced a higher visibility for mariners than a continuous light with the same intensity [9]. Later it was proven that using a blinking light actually yields the best response time for observers and yields a higher conspicuity than static light sources in settings with continuous background lighting [10, 11]. Assuming the product is used in the setting indicated, a blinking light would yield an increase in the conspicuity of the jogger. Additionally, using a blinking light source is expected to require less power on average, due to the decreased amount of time of the light source being operational within the same time frame. Because of the increased conspicuity and decreased power dissipation, a blinking light source will be implemented in the design rather than a continuous light source.

3.3 Light source

Light Emitting Diodes (LEDs) were chosen as the most appropriate light source for the product. LEDs have the advantages of exceptional flux range, unlimited colour control, rapid brightness and colour changes, longest lamp life and the best power conversion efficiency [12, 13]. The exceptional flux range and unlimited colour control leaves a lot of room for optimisation. The rapid brightness changes accommodates blinking of the light source well, especially when considering low duty cycles or (relatively) high frequencies. A long lifetime is important considering the product is intended to remain operational for a long time. The most important factor for choosing LEDs is the power conversion efficiency, due to the very limited power that can be harvested. A major added benefit to the LEDs are their generally small size, as this conforms to the intended minimisation of the size of the product. As for other lighting options, incandescent light sources are considerably less efficient. Most of their energy is converted to heat rather than light and having a wearable product that easily heats up, is far from desirable. Electric discharge lamps, like a compact fluorescent lamp (CFL), generally have larger dimensions than LEDs and are unable to comply with the size constraints of the product. They also lack the colour optimisation and power conversion efficiency of LEDs. Furthermore, LEDs have higher scotopic/photopic ratios than compact fluorescent lamps [14].

3.3.1 LED specifications

There are quite some aspects to be considered when choosing the appropriate LED. Parameters such as correlated colour temperature (CCT), the closely related S/P ratio [15], lifetime, size, luminous efficacy and luminance can be used as selection criteria [16].
The size of the LED should be rather small as to deliver a small product which is less impairing

for the jogger. In consideration of the product's purpose, detection of the light source is of most importance. Luminance is therefore of great importance as this quantity describes the perceived intensity of an object or source. Hence, the luminance should be as high as possible for the available power range. Too high of a luminance could be detrimental to the jogger's own vision, but due to the limited amount of power that is likely to be delivered, it is not expected to be an issue. The lifetime should be sufficient, multiple years, but does not have to be prioritised in the optimisation. For the CCT, a compromise has to be found. High CCT values correlate to increased adaptation time for the eyes to darkness, as well as having a harder time penetrating fog. Low CCT however, will usually also have a lower S/P ratio and therefore worse luminous efficacy in the mesopic vision range [17].

In practice, datasheets of LEDs rarely feature parameters such as CCT, S/P ratio, lifetime, luminous efficacy or luminance. The parameters of CCT and S/P ratio are replaced by LED colour. A study suggests the use of red and yellow coloured LEDs to increase visibility [18], also orange and amber will be considered as viable options, as they lie in between the red and yellow light spectrum. The lack of lifetime information is quite insignificant as LEDs generally have a lifetime of several ten thousands of hours [19]. The datasheets do provide either the typical light intensity or light intensity range, which can be used as replacement for luminance. Further available criteria to use, are the maximum power dissipation (not always shown), viewing angle, forward voltage and forward current. The viewing angle here refers to the angle at which half of the maximum brightness is emitted. The forward voltage is specified with either a minimum, maximum, a typical value or usually as a combination of these. The forward current usually only specifies a maximum and typical value. The power dissipation can be calculated for the typical values or maximum values as a function of the forward current and forward voltage according to Equation 3.1.

$$P = U_{fwd} \cdot I_{fwd} \tag{3.1}$$

With P the power, U_{fwd} the forward voltage and I_{fwd} the forward current. Lastly, an important factor that has yet to be mentioned, is the availability. The components that are available are limited mainly due to time constraints. Using the minimum light intensity value of flashing cycling lights in the United Kingdom, of 4 cd [20], as a reference, a range of 2 cd to 8 cd was used as search criteria after setting a minimum viewing angle of 90°. A list of available LEDs that were considered, can be found in Table A.2. The table features calculated typical and maximum power dissipation according to Equation 3.1. The maximum power dissipation from the datasheet is provided when available. These LEDs were further categorised by typical forward current. The typical forward current was chosen instead of the power due to the typical forward current being specified as either 20 mA, 30 mA, 50 mA, 100 mA and 140 mA compared to fluctuating typical forward voltages, and therefore typical power dissipation. Within these categories the LEDs with the highest light intensity were chosen. No LED was chosen from the 30 mA and 140 mA categories. As the 20 mA features an LED that outclasses the 30 mA LEDs in most aspects (except for the viewing angle). The 140 mA category features a typical power dissipation that is expected to be too high for the product. The three LEDs chosen to be tested in practice are the OVA-1088 (red), the LA G5AP-CZDZ-24-1 (amber) and the LO E67F-BADA-24-1 (orange).

3.4 LED configuration

The LEDs must cover the front and back of the jogger. While having an LED cover an additional side of the jogger is preferable, it is of lesser importance. As explained in Subsection 3.2.3, the LEDs should be blinking. The optimal solution in terms of visibility, would therefore be three alternating LEDs, or more specifically three blinking LEDs with each a duty cycle of 33% alternating between the front, side and back of the jogger. It might be preferable though to decrease the duty cycle in order to save power.

3.5 Driver circuit

The input source provided by the energy conversion group consists of a (partially) charged supercapacitor. The voltage available is about 4.8 V when the supercapacitor is fully charged, but the voltage will drop over time depending on the amount of current drawn according to Equation 3.2. The lights should keep blinking for at least half a minute after the jogger stops. It is therefore of utmost importance to maximise power efficiency, as to deliver as much of the drawn power to the LEDs as possible.

$$I_c = C\frac{dV_c}{dt} \tag{3.2}$$

Initially all LEDs were to be driven by the driver circuit, this would cause the LEDs to not function before the supercapacitor was charged to a certain voltage. Additionally the driver circuit had to draw less power from the supercapacitor than was supplied, as otherwise the driver circuit would oscillate between barely or not operating. Due to these limitations, two of the diodes within the rectifier of the energy conversion circuit were replaced by two LEDs and the LED driver circuit was decoupled from the storage whenever the jogger generates a voltage above a certain threshold. This enables immediate operational LEDs while jogging as well as the LED driver circuit power consumption being only limited by the amount of operating time when not jogging. This also means that two LEDs are present additionally to those within the driver circuit. For more information see the energy conversion and storage group's thesis.

The blinking LED circuit requires the supplied DC-like voltage to be modulated into a rectangular wave that drives the LEDs. Such a circuit is generally referred to as a relaxation oscillator. Multiple options will be covered in the following subsections, of which most will feature some kind of astable multivibrator. An astable multivibrator is a kind of relaxation oscillator that switches continuously between two output states without the need of an external trigger, hence being astable. Only later on was an option considered, that uses an external trigger (Subsection 3.5.8), due to initially expecting such a circuit to be unfeasible. Each subsection will shortly explain the main working principles of the circuit, how the dropping voltage of the supercapacitor influences its behaviour and conclude on its feasibility. If feasible, the possible LED configurations will be described and an additional analysis will be provided using models whenever possible and relevant. These models do not take into account the dropping source voltage of the supercapacitor due to the increased difficulty and available time. The component values used in the models are based on available components and are tuned to achieve a frequency of approximately 2 Hz, which was experimentally determined to be close to a jogger's running frequency.

3.5.1 LED driver IC

Dedicated LED driver integrated circuits (IC) that enable blinking LEDs do exist. However, these circuits operate in power ranges of several watts, while the energy harvester delivers power in the order of milliwatts. These driver ICs are therefore unsuitable for the product.

3.5.2 Breakdown oscillator

The breakdown oscillator circuit, Figure 3.1, features a bipolar junction transistor (BJT) in reverse bias and in parallel with a capacitor. The capacitor charges until the voltage over the capacitor reaches the breakdown voltage of the BJT. When this threshold is reached the transistor starts to conduct current. The capacitor starts to discharge through the transistor. When discharged the voltage over the capacitor and therefore the transistor, has dropped below the breakdown voltage of the BJT again. The BJT stops conducting and the capacitor starts charging again, repeating the process.
The voltage levels needed to drive this circuit are generally in the order of 10 V or higher, which is a lot more than the 4.8 V that is available. Considering the dropping voltage of the supercapacitor this option is unfeasible.

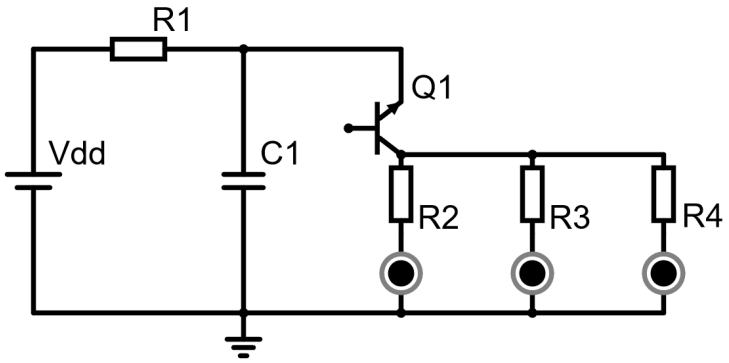

Figure 3.1: Schematic of a breakdown oscillator.

3.5.3 Comparator oscillator

The comparator oscillator circuit, Figure 3.2, features an operational amplifier (op-amp) that acts as a comparator. The op-amp compares the voltage over a capacitor that is connected to the op-amp's output (V^-), with the op-amp's output after a voltage division (V^+). Depending on which is higher, the output will be either low ($V^- > V^+$) or high ($V^- < V^+$). Due to the capacitor charging and discharging, V^- will change and trigger the switching of the output when the threshold $V^- = V^+$ is reached. Achieving two astable output states in the process.
Preferably the output would switch between a positive source voltage and ground, due to the single (positive) voltage source available. This is however, not possible due to V^- having to compare to 0 V, which for the exponential discharge of the capacitor takes infinitely long, as can be deduced from the relation $V^- = V_C e^{-\frac{t}{R_1 C_1}}$. Alternatively, the op-amp could be powered by a positive and negative source voltage. This can be achieved by creating a virtual ground using a voltage divider. This would divide the voltage in half, leaving the LED and resistor at the output with only 2.4 V. Considering that the forward voltage of the chosen LEDs are typically 2.2 V, the LEDs would dim down and stop operating very quickly when the supercapacitor's

voltage drops due to discharging. The voltage divider could be tuned as to have a larger voltage difference between the positive terminal and the virtual ground simultaneously decreasing the difference between the negative terminal and virtual ground. This would allow for higher voltages to drive the LEDs at the output but would consequentially increase the duty cycle and therefore increase the power dissipation by the LEDs. In conclusion the comparator oscillator makes for a feasible but unsuitable implementation.

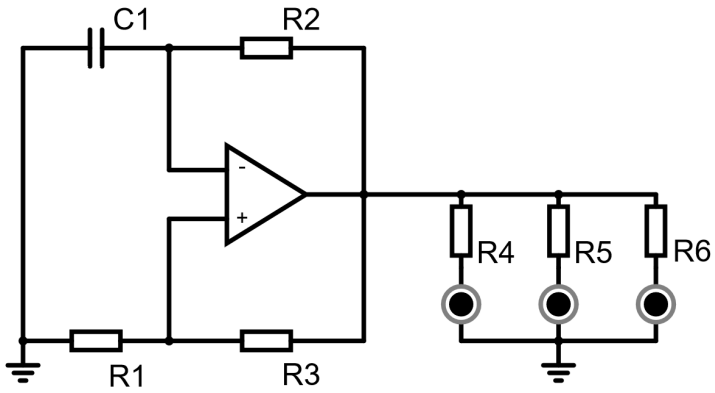

Figure 3.2: Schematic of a comparator oscillator.

3.5.4 Unijunction transistor oscillator

The UJT oscillator, Figure 3.3, features a unijunctional transistor (UJT) that operates as an electronic switch. Initially, when the capacitor is discharged, the UJT doesn't conduct and the capacitor starts charging. When a threshold voltage is reached, the UJT starts to conduct from emitter to the base connected with the LEDs. The capacitor starts to discharge through the LEDs and the process repeats. This implementation is not feasible for the product because a UJT is a too expensive component. They cost about eight euros a piece which would significantly drive up the price of the product. The UJT oscillator is therefore not considered an appropriate option.

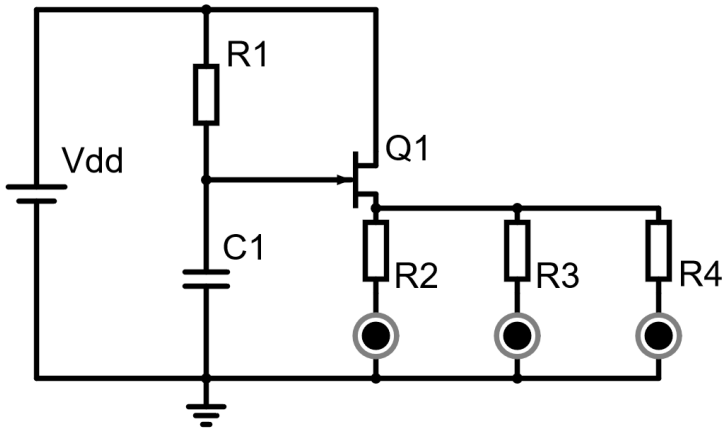

Figure 3.3: Schematic of a unijunction transistor oscillator.

3.5.5 Inverting Schmitt trigger oscillator

The inverting Schmitt trigger oscillator, Figure 3.4a, features an inverting Schmitt trigger that switches between a high and low voltage output depending on its input voltage. It defines the input as being either low or high and adjust its output to be the opposite. The thresholds of the input voltage being high or low differ depending on whether the transition goes from high to low or low to high. The output of the inverter is fed back to the input enabling continuous oscillation at the output. The feedback is delayed using a capacitor in order to control the frequency and the corresponding duty cycle. The inverter is powered by the supercapacitor and the inverter's output nears its source voltage. As the supercapacitor's voltage drops, the thresholds and output voltages change. This reduces both the oscillation time period and decreases the brightness of the LEDs over time. The circuit stops operating when the output of the inverter reaches the forward voltage of the LED.
The inverting Schmitt trigger oscillator is a feasible option. It delivers relatively high voltages to the LED in the high output state and is a rather small circuit, due to the small amount of components.
It can power one or multiple LEDs in parallel and let them blink simultaneously. The duty cycle should be close to 50% due to the same charge and discharge path being used in both output states, hence achieving similar RC times.

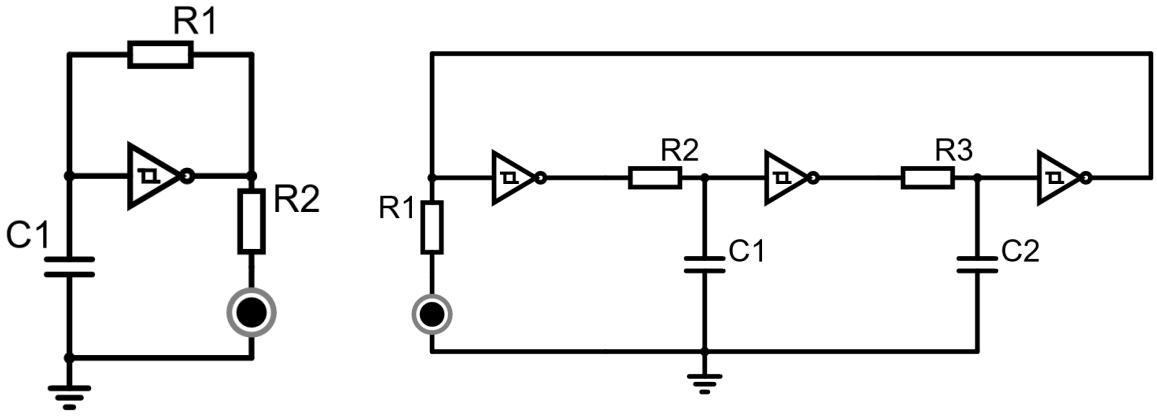

(a) Implementation with one inverter element.

(b) Implementation with three inverter elements.

Figure 3.4: Schematics of a Schmitt trigger oscillator.

Inverting Schmitt trigger model

The inverting Schmitt trigger oscillator circuit has been subjected to circuit analysis from which a model was derived and implemented into a MATLAB script. The model and its corresponding MATLAB script can be found in Appendix C.2 and Appendix D.1 respectively.

In order to validate whether the model behaves as anticipated, four characteristics have been plotted in Figure A.2. It is assumed that at time $t = 0s$ the voltage source is connected to the inverting Schmitt trigger. At this point in time the circuit has only noise present which corresponds to a low input voltage for the inverter, therefore the initial output state of the inverter is determined to be high. The capacitor in the circuit is assumed to have an initial voltage of 0 V as when no energy supply is present, the capacitor can dissipate its stored energy over the resistor. The top left plot in Figure A.2 correctly shows the capacitor charging from 0 V

initially to the low-to-high threshold voltage of the inverter before discharging to the high-to-low threshold voltage. From thereon the capacitor keeps charging and discharging between both thresholds as intended. The top right plot correctly shows the inverter output voltage starting off high and switching the same time as the capacitor reaching the corresponding threshold. The bottom right plot correctly shows that no current flows through one LED when the inverter output is low. A bit less than 15 mA is delivered per LED, this current should achieve a not too great brightness, but still acceptable. The output current of the inverter in the bottom left plot shows approximately three times the amount of current that is delivered per LED when the inverter output is high. When the inverter output is low, the output current shown is approximately zero. The current drawn and delivered by the RC part of the circuit is about 400 times smaller than the combined current drawn from the LEDs and therefore present but barely perceivable on the plot. As expected, this small current is negative when the output of the inverter is low, due to the current discharged by the capacitor flowing back through the inverter. To increase the brightness of the LEDs, the current flowing through them should be increased by decreasing the series resistance. This however, would result in output currents that start to exceed 50 mA, which is the highest absolute maximum rating found for an inverting Schmitt trigger available at our designated distributors [21, 22, 23].

In the top left and top right plots from Figure A.3, the amount of power delivered by the source and the amount that is delivered to the LEDs are shown respectively. The bottom two plots show the time duration of one period and how much time of such a period the LEDs are operating. One time period is defined as the time duration of the inverter output being high and low consecutively, once. The duty cycle is approximately 50% as expected. The most important results from the model are the average amount of power consumed by the entire circuit as well as how much of it was delivered to the LEDs. As these give a comparable representation of the efficiency of the circuit as well as an indication of the LEDs relative brightness. These results are shown in Table A.1 and are discussed in Subsection 3.5.9.

In order to decrease the power consumption while maintaining the brightness of the LEDs, an attempt to reduce the duty cycle of the LEDs was made. This was done by chaining multiple inverting Schmitt triggers with delay elements as in Figure 3.4b. An elaborate model was produced to analyse the effect of chaining multiple (different) elements. These elements consist of either an LED with resistor followed by an inverter, a resistor with capacitor followed by an inverter or a combination of both the LED and capacitor (with corresponding resistors). The results of the model, shown in Figure A.4, revealed that the duty cycle barely changed. This is due to the dependency of each element on the other. Having an element change its output state slower than others only affects the time period by slowing the whole switching process down. As the duty cycle could not be reduced, the power consumption would only go up due to using more components. The script of the model can be found in Appendix D.1.

3.5.6 555 Timer oscillator

The 555 Timer oscillator (Figure 3.5), features a 555 timer IC that can be operated in an astable state producing a square wave. Initially the capacitors are uncharged and therefore the voltage over the capacitors is 0 V. The output of the IC is high whenever the voltage at the trigger pin is below one third of the source voltage. As the trigger pin is connected to the upper plate of the capacitor C_1, that starts off at 0 V, the initial output state of the IC is high. When the threshold pin, also connected to the upper plate of C_1, reaches two thirds of the source voltage, the output drops to the low output state. This threshold is reached due to the charging of the capacitor

through resistors R_1 and R_2. The discharge pin, connected between resistor R_1 and R_2, shorts to ground whenever the output state is low. Therefore, the capacitor discharges through R_2 whenever the output is low. This causes the capacitor's voltage to oscillate between one third and two thirds of the source voltage, with the output consequentially oscillating with it. The control pin allows to change the threshold of the threshold pin. When unused, as in this case, it is connected to a very small capacitor as to keep the standard threshold while not allowing current to flow through. As the voltage over the supercapacitor drops, the threshold and output voltages change. This decreases the oscillation time period and reduces the brightness of the LEDs. When the output voltage of the IC reaches the forward voltage of the LED, light will no longer be emitted.
Due to the limited availability of 555 timer ICs that are able to operate with lower voltages than 5 V, it is considered a less feasible option compared to similar implementations.
The implementation could drive one or multiple LEDs blinking simultaneously in a parallel configuration.

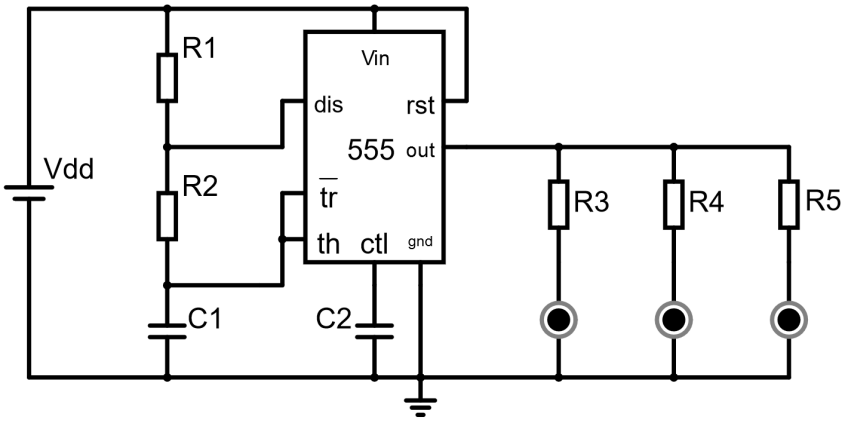

Figure 3.5: Schematic of a 555 Timer oscillator.

3.5.7 Bipolar junction transistor oscillator

The bipolar junction transistor (BJT) oscillator, shown in Figure 3.6, features two BJTs that operate as switches. Initially both transistors are turned off (no conduction) and the base emitter voltage (V_{be}) of both these transistors start to rise. One V_{be} will reach the threshold voltage of the transistor earlier than the other due to small physical imbalances in the circuit. Transistor Q_1 is assumed to conduct first, with transistor Q_2 turned off. With Q_1 conducting, the current emitter voltage (V_{ce}) of Q_1 drops to 0 V. As Q_2 does not conduct, the capacitor C_2 will charge due to the current flow through resistor R_4. When fully charged V_{ce} of Q_2 reaches the source voltage, which happens quickly due to the resistance of R_4 typically being very small. As V_{be} of Q_1 remains at the threshold voltage, the potential over C_2 will be the difference between the source voltage and the threshold voltage. While Q_1 conducts capacitor C_1 is charged due to the current flow through resistor R_2. As the capacitor charges and V_{be} of Q_2 reaches the threshold voltage, Q_2 will start to conduct. This pulls V_{ce} of Q_2 down to 0 V and due to the potential over the charged capacitor, V_{be} changes to the negative difference of the source voltage and the threshold voltage. This turns Q_1 off, mirroring the process. This astable process produces a square wave output at both V_{ce} with one being the inverse of the other.
There are two locations that the LEDs could be connected to, in order to drive them with a

square wave. The first option, depicted in Figure A.5a, has an LED placed between the resistor and the transistor's collector beneath it. The main issue of this implementation is that the necessary forward voltage for the LED to conduct significantly reduces the potential that can be build up over the capacitor when the transistor in that branch is off. The lower that potential is, the less time is required for the corresponding V_{be} to reach the threshold voltage. Therefore, using this implementation significantly increases the frequency of switching.
The second option, depicted in Figure A.5b, connects the LED between the collector of the transistor and ground. The explanation on the additional branch will be momentarily postponed. This implementation drives the LED whenever the corresponding transistor is off and the capacitor above it charged. This consequentially means that current flows that were previously impossible due to the non-conducting transistor, are now flowing through the LED. This significantly drives up power consumption and reduces the percentage of power delivered to the LEDs. The potential over the capacitor can be charged up until the forward voltage of the LED. The lower the source voltage is, the more of an improvement this becomes over the previous implementation.
As shown in Figure A.5b, the BJT oscillator can be extended to accommodate for a third LED. The operating principles of the circuit remains the same but in this case two of the transistors conduct.
For both the series and parallel LED implementation, the duty cycle will be 50% per LED if $R_1 = R_4$ and $R_2 = R_3$. The resistor values can be tuned to increase the duty cycle of one LED and consequentially decrease the duty cycle of the other, but this has no added benefits when considering power consumption. When the parallel LED implementation is used with the third branch, the duty cycle (with balanced resistor values) will be one third per LED instead. This has the benefit of driving three alternating LEDs but adds power consumption due to the additional current flows through the additional transistor.
These implementations are feasible but far from ideal. Both two and three parallel branch LED implementations are highly inefficient when it comes to power delivered to the LEDs. The series LED implementation should be quite efficient, but struggles with low voltages, as the frequency will quickly rise when the source voltage nears the LED's forward voltage. As the voltage source in question is a supercapacitor whose voltage drops as it discharges, this becomes a significant issue.

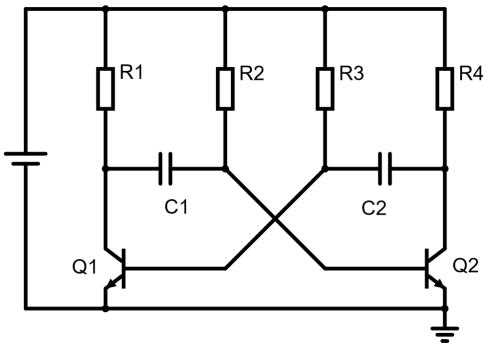

Figure 3.6: Schematic of a bipolar junction transistor oscillator.

BJT oscillator model

A model of the parallel LED implementation of a BJT oscillator with two branches, was designed and implemented in MATLAB. The model and its corresponding MATLAB script can be found in Appendix C.3 and Appendix D.2 respectively.

The model assumes that the circuit has been operational, with at time $t = 0$ transistor Q_1 having been switched on and transistor Q_2 having been switched off.

Figure A.6 validates that the model behaves according to the theory it was based upon. The top left plot of Figure A.6 correctly shows how each cycle, one base emitter voltage rises towards the switching threshold from the negative potential of the capacitor, while the other stays at the threshold. The top right plot correctly shows how each cycle the collector emitter voltage of the transistors switches from 0 V to the forward voltage of the LED. This corresponds with the transistor conducting at 0 V and being turned off when the voltage starts to rapidly rise or remains at the LED's forward voltage. The bottom right plot shows the current that is delivered to both LEDs. Consistently one LED has current flowing through, with the exception of the near instantaneous peaks present in the plot. These represent the very short period of time in which the capacitor needs to be charged to the forward voltage of the LED after the corresponding transistor has been turned off. The bottom right plot shows the current drawn by the entire circuit. It has similar but inverse peaks compared to the current through the LEDs, which represents the extra current drawn for the same charging of the capacitor. Besides these peaks the current is mostly constant which is to be expected due to the symmetry in the circuit.

The plots from Figure A.7 give insight into the performance of the modelled circuit. The power delivered by the source, shown in the upper left plot, shows the same characteristic as the closely related current drawn by the circuit. Similarly the power delivered to LEDs, shown in the top right plot, features the same characteristics as the current delivered to the LEDs. For further insight into the performance in terms of power, the average power drawn by the circuit, the average power delivered to the LEDs and the ratio between the two have been calculated. These results are shown in Table A.1 and will be discussed in Subsection 3.5.9.

3.5.8 4017 clocked decade counter circuit

The 4017 clocked decade counter circuit, shown in Figure 3.7, features a clocked decade counter/divider integrated circuit (IC). The 4017 IC, Figure A.10, has ten output pins of which one outputs a voltage close to the supply voltage, while the others are pulled to ground. When the voltage connected to the clock pin rises from low to high, the output shifts to the next pin. The clock signal is generated using two NAND gates that act as an inverter, in combination with a capacitor. The NAND gate always has the inverse output of the other NAND gate because of their inputs being connected to the other's output. The constant switching of two chained NAND gates is slowed down by the charging of the capacitor. The frequency of switching is controlled by C_1's capacitance and R_1's resistance. The clock signal is synonymous with the output signal of NAND $U1 : B$, as it is directly connected to the clock pin. The reset and clock inhibit pins are connected to ground to make sure that the counter does not reset or stop switching outputs. Three outputs are connected to an LED in series with a resistor. This resistor limits the output current of the IC to protect the LEDs and IC from damage due to currents exceeding their maximum ratings. As the voltage of the supercapacitor drops, the threshold and output voltages of the NANDs as well as the output voltage of the 4017 IC changes. As a consequence the frequency of the clock signal will increase and the LEDs will decrease in brightness and completely dim down when the output voltage equals the forward voltage of the LED.
Considering the preference for the use of three LEDs, two configurations are considered. The three LEDs could be connected to output pin 0 up until 2 with output pin 3 connected to the reset. This will give the LEDs a duty cycle of one third each, which in practice will be a bit less due to the delay when resetting. Alternatively the LEDs could be spaced out over the ten

pins. This achieves a duty cycle of a tenth per LED. Due to the importance of efficient power dissipation, the second options seems more feasible as it features less LED operation time and therefore less power dissipation.
This circuit seems very feasible due to the low expected power consumption as well as the preferred three alternating LEDs.

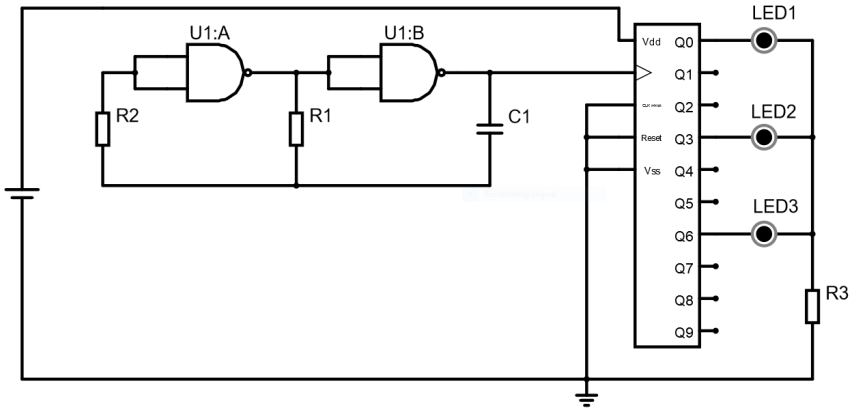

Figure 3.7: Schematic of a 4017 chaser using a NAND gate clock and driving 3 LEDs.

Clocked decade counter circuit model

A model of the 4017 clocked decade counter circuit was designed and implemented in MATLAB. The model and its corresponding MATLAB script can be found in Appendix C.4 and Appendix D.3 respectively. This model assumes that at time $t = 0$ NAND $U1 : A$ has a high output and NAND $U1 : B$ a low output. The capacitor is initially uncharged and therefore has a potential of 0 V.

The plots in Figure A.8 show how the modelled circuit behaves when operational. The top left plot shows the voltage over capacitor C_1. The plot shows how the capacitor charges and discharges towards the output between the NAND's high threshold voltage (negative) and the difference between the NAND's high output and low threshold voltage (positive). Whenever NAND $U1 : B$'s output voltage shifts from low to high, the IC's output shifts to the next pin. The top right plot shows the current drawn by the oscillator. It oscillates with the switching of the NAND gates and its amplitude is relatively low. The bottom left plot shows the current delivered to the LEDs. Notice how after every pulse there are twice as long down times, with the exception for every third pulse which has thrice as long of a down time. This perfectly corresponds to the pins that these LEDs are connected to, as the first pulse corresponds to the LED at the first pin followed by two empty pins. The second pulse corresponds with the LED at the fourth pin followed by two empty pins and the third pulse corresponds to the seventh pin followed by three empty pins. The bottom right plot shows the current drawn from the source by the entire circuit. It predominantly consists of the current drawn by the LED which is favourable considering the source is a supercapacitor that decreases in voltage as more current is drawn.

The plots in Figure A.9 show the distribution of power usage of the circuitry. The top left plot shows the power drawn from the source by the oscillatory circuit. The shape of the signal is similar to the current drawn by the oscillatory circuit as expected. The top right plot shows the power drawn by the IC, LED and resistor R_3. It correctly follows the switching sequence of the pins and does not dissipate power when the output does not have an LED connected. It draws significantly more power compared to the oscillator, which is better observed in the bottom left

plot that shows the total amount of power drawn from the source. This is to be expected as the oscillator requires a lower current to operate. The bottom right plot shows the power that is delivered to the LEDs. When compared with the top right plot, the power dissipated by the LEDs is less than half. Most is lost to the current limiting resistor that is placed in series with the LEDs, which cannot really be circumvented as allowing more current would be harmful for the components. The oscillation period of this model is $T = 0.5065s$, while the duty cycle for each LED is 10% assuming that the oscillatory signal does not change over time. Other parameters, such as the average power dissipated, can be found in Table A.1, where they will be compared to those of different models.

3.5.9 Comparison

When comparing the LED driver circuit models in Table A.1, the clocked decade counter model comes out on top. The average power it dissipates is far less than the others, even if the combined duty cycle would be increased to a similar value of the other models by adding LEDs to the circuit. This can be extrapolated from Figure A.9, as it shows that the circuitry that dissipates power regardless of LED operation is inconsequential compared to the power dissipation of the LED and corresponding resistor. So adding additional LEDs will increase the average power almost linearly. The model is the second most efficient in terms of delivering power to the LED, right behind the inverting Schmitt trigger. It is more restricted in terms of supplied LED current than the BJT oscillator due to the absolute maximum ratings on the IC. This reduces the potential brightness of the LEDs, it is however a minor trade-off considering the BJT oscillator discharges the supercapacitor that much more quickly. For these reasons has the 4017 clocked decade counter circuit been chosen.

3.6 3D design

To design the case and the energy harvesting tube knowledge of 3D modelling was needed. The program that was used for 3D modelling is Fusion 360, as this program was recommended for beginners. The necessary skills for using this program were gained after many hours of trial and error.

3.6.1 Energy harvesting tube

The energy harvesting group required some sort of tube in order to do tests on magnets moving through a coil. The tube needed to be hollow for the magnet to properly move through, and have an area which the coil can easily be wound on. It should be possible to place smaller magnets on the top and bottom of the tube, which will repel the magnet inside the tube. The design started with a simple hollow tube with an inner diameter of 11.00 mm and an outer diameter of 14.00 mm, see Figure 3.8a. A base plate was added at the bottom, with an outer diameter of 30.00 mm, so it can be held more easily. This plate was chamfered at an angle of 45° for better printing results, because a printer cannot print something which is floating in the air. Subsequently two disks were added in the middle of the pipe with a distance of 15.00 mm between them, where the coil can be wound. One of these disks is also chamfered at an angle of 45° for printing stability, but the other is not, because it would interfere with the location of the coil. So the other disk is just perpendicular to the tube, which means support has to be added while printing, and cut away when done. A separate lid was designed in order to close off the tube. This lid has a circle at the bottom, which has an outer diameter of 10.50 mm and stands out 1.50 mm, so it will fit on the tube and stay in place.

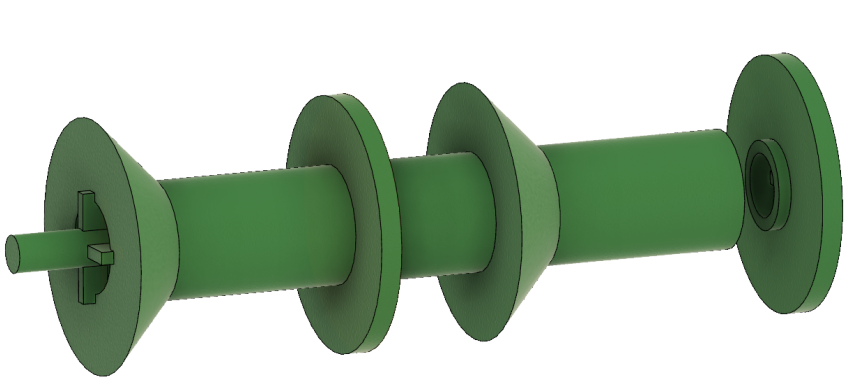

(a) Model of the side view of the tube.

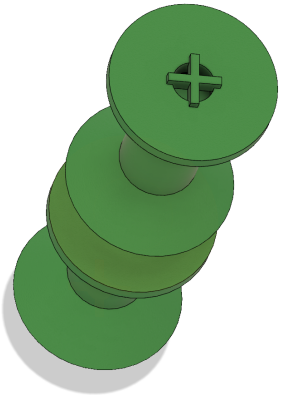

(b) Model of the top side view of the tube.

Figure 3.8

Both the bottom and the lid have an air hole, so the magnets inside the tube can move freely and won't be obstructed by compressed air. These holes are reinforced by crosses, so the magnets won't fly out of the tube. These crosses are also lifted by 1.50 mm, so when the smaller magnets are placed on the outside of the tube they won't seal it off and cause the air to be compressed anyways, see Figure 3.8b. Finally the bottom is fitted with a rod which sticks out 10.00 mm. This rod is specifically meant for the tube to be placed on a hand drill, to make the winding of the coil faster, and will be cut off when the coil is made.

A second version of the tube was designed once more information became available from the other two groups and the faults of the first prototype were analysed, see Figure 3.9. To make the energy harvester more efficient the distance between the magnet and the coil had to be minimised, so the inner diameter of the tube has been reduced to 10.40 mm, and the outer diameter to 12.40 mm. This inner diameter is just enough for the magnet to move freely inside of the tube while the tube wall cannot be made smaller than 1.00 mm, otherwise it won't be strong enough, so the outer diameter has to be 2.00 mm bigger than the inner diameter. The disks in between which the coil is wound still have a diameter of 30.00 mm to be able to contain the amount of windings needed. The reinforcement crosses in the bottom and the lid have notches of a 5.20 mm diameter and 2.00 mm depth, so the smaller magnets can be held in place. The lid now will enclose the tube on the outside, instead of having a circle on the inside of the tube, because a circle on the inside will shorten the magnet's path inside the tube. At last the rod at the bottom has been removed and replaced with a stand-alone drillbit, which can be stuck in the tube, so the windings can still be wound with a hand drill and the drillbit can be reused instead of the rod, which had to be cut off after one-time use. This design of the energy harvesting tube will also be used in the final prototype.

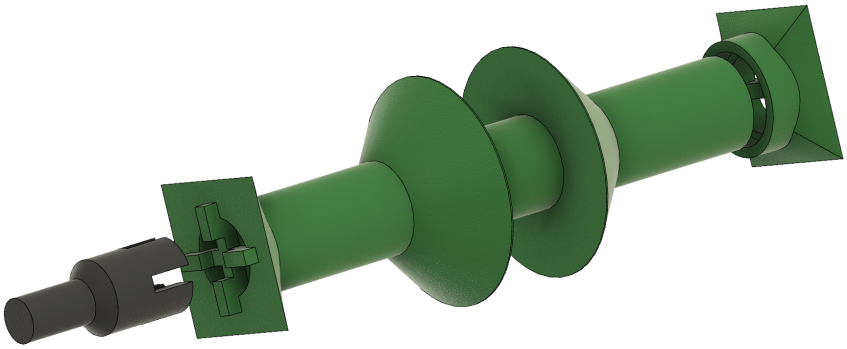

Figure 3.9: Model of the final version of the energy harvesting tube.

3.6.2 Case

Designing the case in an early stage of the project is tricky, as many parameters could still change. The casing should encapsulate the energy harvesting tube and the circuitry of the conversion, storage and lighting, which is soldered on a PCB. A box was designed with compartments for both these components, see Fig. 3.10. The case has an outer width of 77.00 mm, height of 52.00 mm and depth of 26.00 mm without the lid, the lid has a thickness of 3.00 mm. The inner walls have a thickness of 3.00 mm, so a groove of 1.00 mm can be implemented in which the PCB can be slid. These parameters were based on the expectation of having a harvesting tube which is 50 mm long and a PCB which is 50 mm by 50 mm. In the lid and at the side of the case holes are hollowed out for screws, so the lid can be opened and closed easily. Protruding ledges are made on the lid, so it fits more securely.

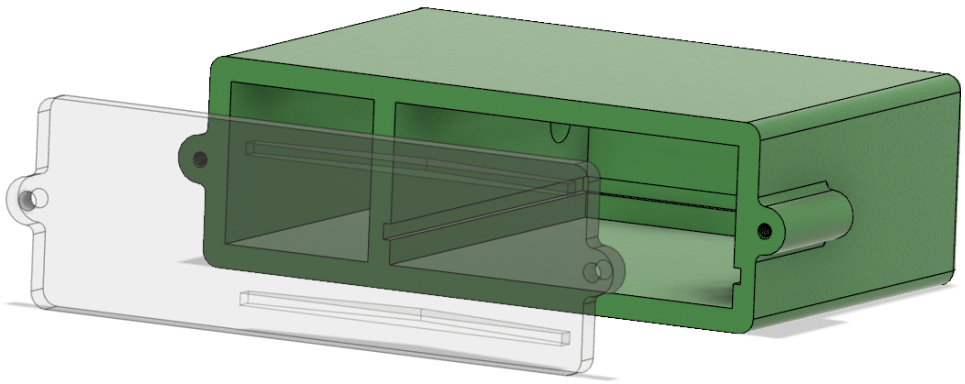

Figure 3.10: Model of the first design iteration of the case.

Later more information about the dimensions of the other components became available form the other groups and a second version of the casing was designed. It still has two compartments, one for the energy harvesting tube and one for the energy conversion PCB, see Fig. 3.11. The dimensions are changed, this case has an outer width of 48.00 mm, height of 83.00 mm and depth of 25.00 mm without the lid, the lid has a thickness of 3.00 mm. These dimensions should be more in line with the arm and consequently the comfort should be increased. The thickness of the walls of the energy harvesting compartment is 2.00 mm and for the circuitry compartment it is 3.00 mm, which allows a groove of 1.00 mm to be implemented. To secure the lid on the case M4 bolts and nuts will be used. In the lid and at the side of the case, holes are formed in which M4 bolts fit, and at the bottom of the hole a slot is designed for an M4 nut, see Fig.

3.12b. A clip was made on the back so the case can be attached on a band, see Fig. 3.12a. The clip has ridges to secure the case better on the band. Three holes are made on the outside where the LEDs should come and two holes in between the compartments for the wiring.

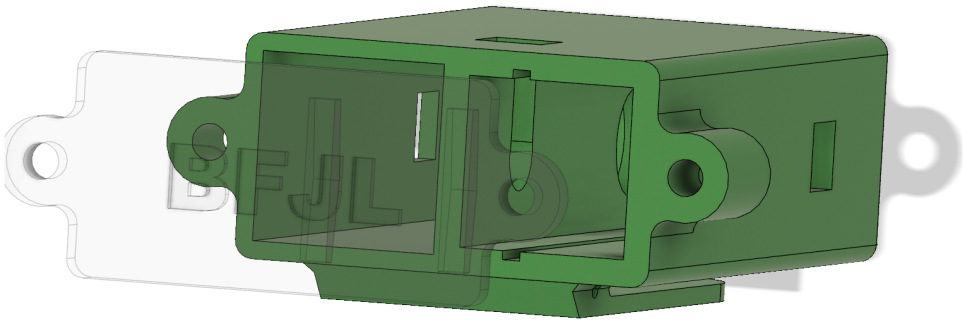

Figure 3.11: Model of the second design iteration of the case.

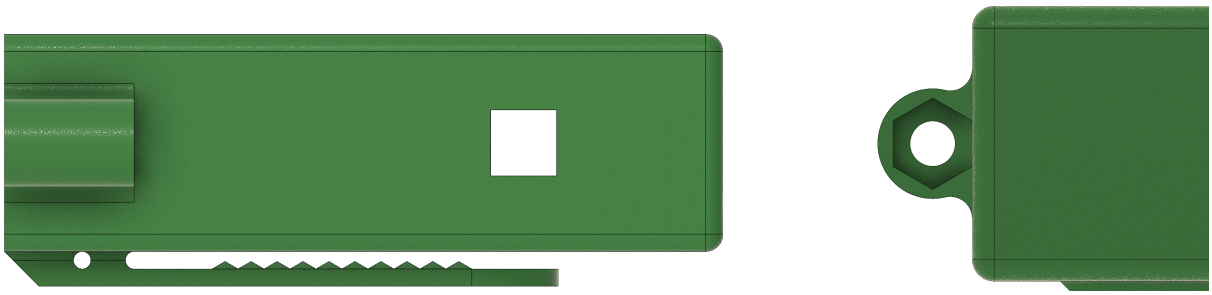

(a) Model of the side view of the case.

(b) Model of the case with a slot for a M4 nut.

Figure 3.12

A final version of the case was designed when the definitive dimensions of the components of the other groups were known. The final version is quite like the second version, but with different dimensions. The final version has an outer width of 54.00 mm, height of 88.00 mm and depth of 34.00 mm without the lid, the lid has a thickness of 3.00 mm, see Figure 3.13. So it has gotten bigger than the second version, but this is needed as the energy harvester has a bigger diameter than was expected beforehand, due to an increase in windings. The clip and the holes for the M4 bolts and nuts haven't changed. The thickness of the walls of the energy harvesting compartment is still 2.00 mm and for the circuitry compartment still 3.00 mm. Grooves in the shape of a cross as well as side banks have been added in the bottom and the lid, so the energy harvesting tube cannot turn around inside the casing, see Figure 3.14a. The cross-shaped grooves are 1.00 mm deep and the side banks protrude 4.00 mm. On the lid the side banks are made in the form of protruding ledges, which have a double function. These protruding ledges secure the lid in position on the case and make sure the lid of the tube cannot turn around. The grooves in which the PCB will be slid are now 1.50 mm deep, so it will fit more securely. In the case cut-outs are made for the LEDs. It was decided to use five LEDs, so in comparison to the second version of the case, more holes needed to be created to fit them in the case. The LEDs will be soldered on small pieces of circuit board, the cut-outs are 1.00 mm deep and have an area of 10.40 mm by 12.70 mm or 20.40 mm by 12.70 mm, depending if one or two LEDs are soldered on the board. Holes are made in the cut-outs to the outside of the case measuring 7.70

mm by 5.20 mm through which the LEDs will be sticking out. On each side of the casing there are holes for two LEDs, so the jogger has light to his/her front and back while jogging. At the front side of the casing there is a hole for only one LED, so when standing still the jogger has flashing lights to the the back, side and front, because, as discussed in Chapter 3.2.1, only at junctions should the jogger ever be approached from his/her side.

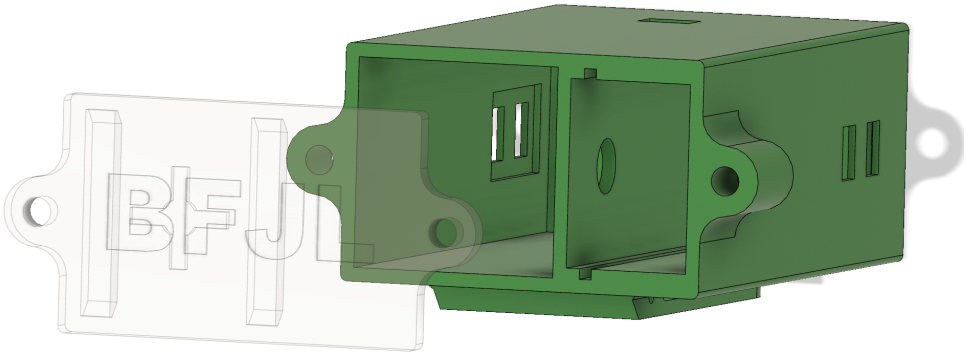

Figure 3.13: Model of the final design of the case.

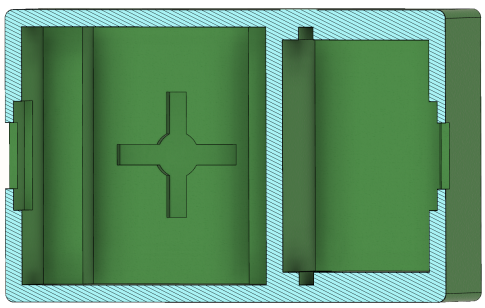

(a) Model of the case with grooves for holding the energy harvesting tube and the PCB in place.

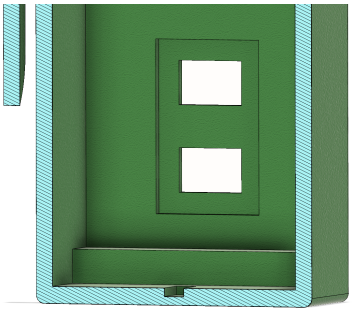

(b) Model of the case with cut-outs for the LEDs placement.

Figure 3.14

Chapter 4

Prototype

4.1 Circuitry

While models were made for the LED driver circuits, the most likely candidates were also being implemented and tested in parallel. This was due to the energy conversion and storage group requiring the circuits as soon as possible for load testing (see Appendix B for further elaboration on group dynamics). The inverting Schmitt trigger circuit was not tested; the implementation required the use of special equipment for small scale soldering, which also required more time to effectively use. On the other hand, the BJT oscillator easier to implement due to all components being readily available and convenient to use. The BJT oscillator was therefore implemented and tested first and by the time this was done, the analysis of the circuits concluded on using the 4017 clocked decade counter circuit. The implementation and testing of the inverting Schmitt trigger circuit was therefore skipped entirely and the 4017 clocked decade counter circuit was implemented and tested instead. The results from testing the BJT oscillator, though not entirely relevant for the final prototype, are mentioned due to the BJT circuit's unexpected behaviour.

4.1.1 BJT oscillator

The BJT oscillator was built according to Figure A.5a. When tested, the circuit behaved highly imbalanced; one LED was on for a significantly longer time than the other. The voltage over the LEDs is shown in Figure A.11. The duty cycles were estimated to be about 15% and 85%. This happens due to the voltage over V_{ce} charging up significantly slower for one branch compared to the other when that branch's transistor is not conducting. The plot would suggest that the forward voltage of the LEDs greatly differs, as the voltage when the transistor is not conducting has such a difference. The voltage at V_{ce} should be able to charge up, until it reaches the difference between the source voltage and the minimum forward voltage of the LED, as no voltage difference will exist over the resistor, hence no current would flow that could charge the capacitor. So the minimum voltage present over the LED should be its minimum forward voltage. However, when only the LEDs where switched around the skewed duty cycle remained present at the same branch. The circuit was tested with components switched around with little to no effect. It is therefore likely that problem originates from the wiring and connections but no conclusive evidence for this causation was found.
When connecting the circuit to a fully charged supercapacitor, the frequency did increase as voltage decreased. This did validate the expected effects.

4.1.2 4017 clocked decade counter circuit

The 4017 clocked decade counter circuit was build and tested according to the schematic of Figure 3.7. Information on the components and their corresponding values can be found in Table A.3.
The period T, consisting of 10 NAND oscillator clock cycles, was modelled to be $0.507s$. In reality the clock signal plot of Figure A.12 shows $T = 0.55s$, with clock cycles of $t_{NAND} = 55ms$.

As no strict requirements are set for the frequency, a deviation of about 10% is insignificant. In the middle plot of Figure A.12 the voltage over the LED at output pin 0 is shown. Things to note are the expected duty cycle of 10% and the negative voltages present whenever the other LEDs at output pin 3 and 6 have a high output. This negative voltage is caused by the LEDs having their outputs connected while one has high output voltage at the input and the other 0 V, giving the LED a potential equal to the difference of the forward voltage of the active LED and the high output voltage. This negative voltage has no impact on the LEDs as it does not reach the absolute maximum rating for reverse biasing the LED. Tests were done with different values of R_3 as to either increase the brightness of the LEDs or decrease the load on the supercapacitor in order to increase the operational time of the circuit. The results can be seen in Table A.4. These tests were done with the 4017 circuit connected to the output of the energy conversion circuit with a supercapacitor of 0.1 F and the discharge times from 4.8 V to 2.0 V were timed. Do note that the peak current that was measured, was highly inaccurate due to observing the voltage over the resistor at the moment of switching with an oscilloscope. As the initial voltage drops very quickly, the sample speed of the oscilloscope plays a rather significant role. A resistance of 46.9 Ω was chosen as it has a good trade-off between discharge time and peak current.

4.1.3 LEDs

The LEDs were empirically tested on light intensity, due to the lack of light intensity measurement equipment. After testing the three different LEDs, it became apparent that the amber coloured LA G5AP-CZDZ-24-1 had the best performance even for lower end currents and voltages. The red coloured OVA-1088 had bigger dimensions and were therefore easier to implement into the casing. They however were no longer available after the initial purchase leaving us to work with 5 of them. One broke down and as five LEDs are needed for the design, these LEDs were therefore entirely left out of consideration. The orange coloured LO E67F-BADA-24-1 was generally less bright than the amber LED and also less convenient in use due to its very small size. The amber coloured LEDs were chosen. These LEDs are relatively small, 3.60 mm by 3.40 mm, but can be soldered by hand, and these LEDs were ordered in a large number, so five of them can be used in the prototype.
The light intensity, though unmeasured, is likely to be below four candela as the light intensity of the amber coloured LEDs is between 3.9 cd and 7.1 cd for a current of 100 mA, while the peak current in our application is approximately 29 mA. By doing tests with running in dark environments, it was concluded that the light intensity was of sufficient intensity for this product. To apply these LEDs in the case they were soldered on a small piece of circuit board of 12.50 mm by 10.00 mm. These pieces of solder board are in both dimensions bigger than the LEDs, so the LEDs can be soldered in the middle and the edges can be glued to the inside of the case.

4.2 3D printing

For prototyping it is easier and faster to 3D print the casing instead of mass-producing it in ABS plastic. ABS is a high impact composite material based on a thermoplastic matrix and a particulate rubber phase. It has an excellent balance of properties, due to its two phase nature. ABS is considered as an engineering plastic, which gained its most significant advantage over polystyrene by incorporating rubber, which transformed it from a brittle organic gloss into a ductile thermoplastic with high impact strength [24]. These properties make ABS a very suitable material for the casing. ABS plastic can also be 3D-printed, but cheaper plastics with better characteristics are available, such as polylactic acid (PLA) or Polyethylene terephthalate glycol-

modified (PETG). PLA is just cheaper, but PETG also has higher thermal, impact, chemical and moisture resistance in comparison to 3D-printed ABS. However, as the prototypes just need to be cheap and quickly made, the choice was made to use PLA for the energy harvesting tube, this was recommended by the company printing the prototypes, 3Delft. For the case PETG was chosen, because the case needed to be more durable.

4.2.1 Energy harvesting tube

The first printed prototype tube failed. The design of the tube wasn't inspected correctly before printing, which resulted in chamfered disks that were hollow on the inside. This detail was not noticed, but meant that the tube had indentations on the inside and the magnet could get stuck in the chamfered disks. So this had to be adjusted and printed again. In the second version, see Figure 4.1a, the chamfered disks were filled up, so the tube was smooth all the way on the inside.

The second prototype, Figure 4.1b, also didn't go without troubles. The tube was printed too narrow the first time, so the magnets didn't fit inside the tube. A few settings were changed on the printer, so the second time the tube was printed correctly and the magnets could move freely inside the tube.

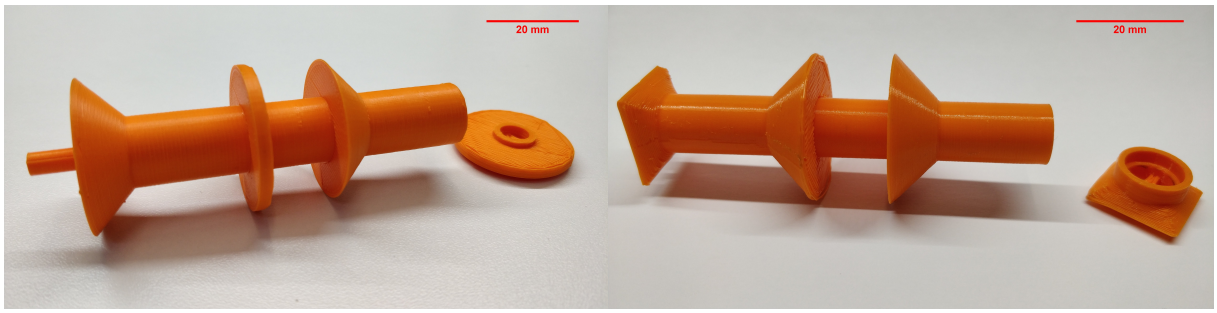

(a) **(b)**

Figure 4.1: Photos of the first (a) and second (b) iteration of the 3D printed tube prototype.

4.2.2 Case

The case was, as mentioned before, printed out of PETG instead of PLA, to make it stronger and more durable. However, the clip had broken off within a minute of having the case in possession. The breaking of the clip was caused by an accumulation of different factors. The material of the clip was still not strong enough and the design was too thin to use as a clip on a belt. A further cause was the way the prototype was printed, as the printer moves horizontally and the layers are stacked up vertically the clip was broken on a horizontal print layer. This was fixed by gluing a small metal plate to the broken clip of the case, this makes it very sturdy, see Figure 4.2. Fitting the LEDs, PCB and energy harvester inside the case was a tough job, as the case was not designed for assembly. Just enough room was available for all the components, but this made it very hard to place them in the case. However, after a day of doing fine needlework everything was placed in the case and the final prototype worked. The total weight of the case is 158 grams and by hanging it by the new metal clip it is wearable and perfectly usable for joggers. However, it is not waterproof because of the LEDs sticking out of the case.

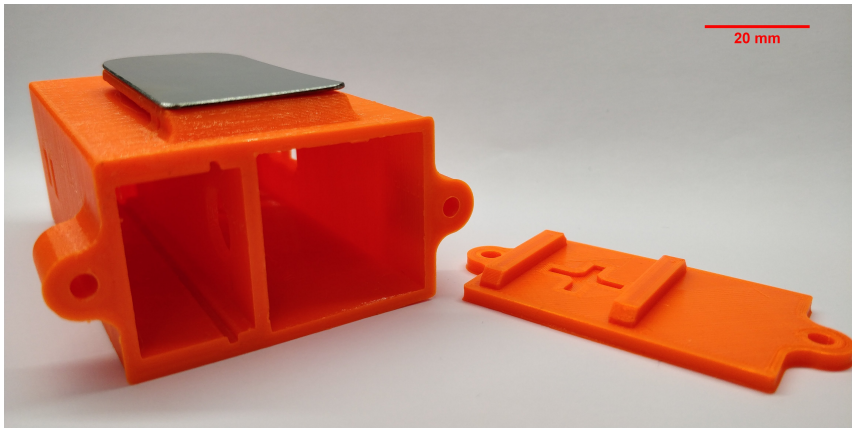

Figure 4.2: Photo of the final prototype of the 3D printed case.

Chapter 5

Discussion

Though the final prototype achieves the intended purpose of providing joggers with increased conspicuity by using blinking lights, while avoiding the use of batteries, not all requirements specified in Chapter 2 have been fully met. While jogging, the frequency of the blinking LEDs is dependent on the frequency of the jogger's movement due to these LEDs being present in a rectifier. However, when the jogger is inactive the frequency of the blinking LEDs is dependent on the LED driver circuit and therefore independent of the jogger's movement frequency. This partially achieved requirement is unavoidable as long as it is undesirable for the operation of the LEDs to be dependant on the charging of the supercapacitor at all times. An angle of visibility higher than the minimum of 180° is achieved at all time, whether the jogger is running, LEDs covering the front and back, or stagnant, LEDs covering the front, back and one side. The light intensity is unmeasured due to lack of measurement equipment. Though the light intensity is likely to be below 4 cd, it is still deemed to be suitable for our product. The value of 4 cd was referenced from cycling lights in the United Kingdom. As cyclist generally share the road with cars more often than joggers, their light intensity should be higher for earlier detection.

The circuit used in the final prototype works as it was designed. Only the clock time differs in the prototype 10% from the designed circuit, this is due to little deviations in the real values of components compared to their supposed values. The final prototype is a bit bulky, as the dimensions are exceeding the limits set up, which was a depth of 2.5 cm. The case has a depth of 3.4 cm, but this was necessary to fit the energy harvester inside the case. Nevertheless has the casing a total weight of 158 grams, which makes it quite lightweight. By hanging the product on either a band on the arm or a belt around the waist with the clip it is wearable and perfectly usable for a jogger. The prototype is not obstructing the movement of the jogger and it is also not harmful for the jogger in any way. The case is however not yet waterproof, this is mostly because of the LEDs sticking out of the case and the lid not fully sealing the case. In the end no specific band or belt has been made, but rather an existing one was used due to priority in time usage.

So most of the requirements set up were a bit too optimistic, nonetheless is it still possible to achieve them. If more time and better resources were available the final product could get more efficient, smaller and waterproof, which makes it more suitable as a jogger light. Some requirements not met could be easily fixed when the product will be mass produced and the case will be injection molded. The waterproofing can be done by using a piece of transparent plastic to cover the LEDs and properly sealing the case. After some optimisation it should be possible to make the case a lot smaller, yet better designed for assembly. The criteria of the maximum cost for the final prototype was also not very realistic. The 3D printing of the energy harvesting tube costs about €12 and the case €26, the production of a single PCB was about €45. So a limit of €100 would be more realistic.

For information on how the group functioned see Appendix B.

Chapter 6

Conclusion

The goal of this Bachelor Graduation Project was to design a jogger light without the use of any batteries. This thesis has focused on the lighting and the casing of the Battery Free Jogger Light. To maximise the visibility of the jogger the product should be placed on the upper part of the body. By making the lights flashing the visibility is increased in dark situations compared to a steady light. The lights used in the product are light emitting diodes (LEDs), as they are the most energy efficient form of lighting in small formats. In the product five LEDs are used, of which two are placed in the rectifier bridge and three are driven by a circuit designed to make the LEDs blink in a chasing way. For this circuit two NAND gates are used to generate a clock signal which switches the states of a 4017 IC. The 4017 IC connects the source to the LEDs one at a time.
All the designed components had to be bundled into a single package, so a case was created in which the energy harvester, the PCB and the LEDs can fit together and make the product work as a whole. Both the energy harvester and the case were designed in 3D modelling software and 3D printed.
The final prototype can be hung on either the upper arm or the waist of the jogger. It functions as it is supposed to and can surely be used by joggers to increase their conspicuity in dark environments while jogging.

Appendix A

Tables & Figures

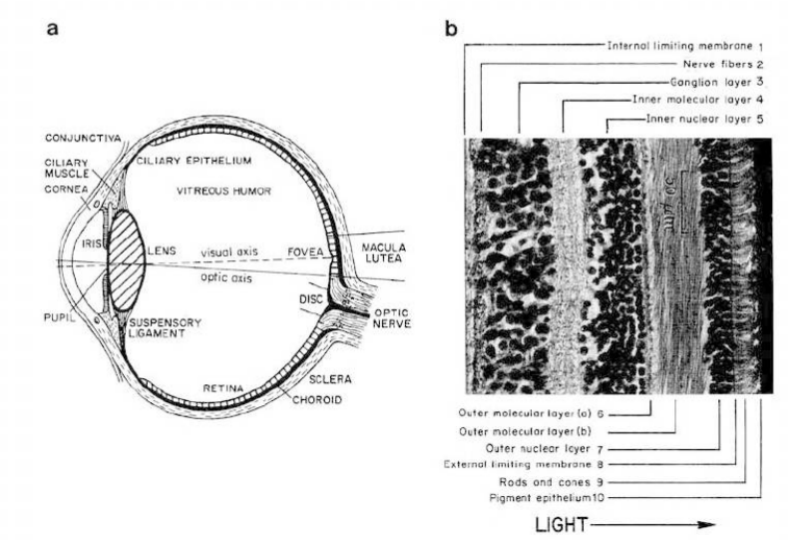

Figure A.1: (a) Structure of the vertebrate mammalian eye. (b) Various cell layers in the human retina (from [25]).

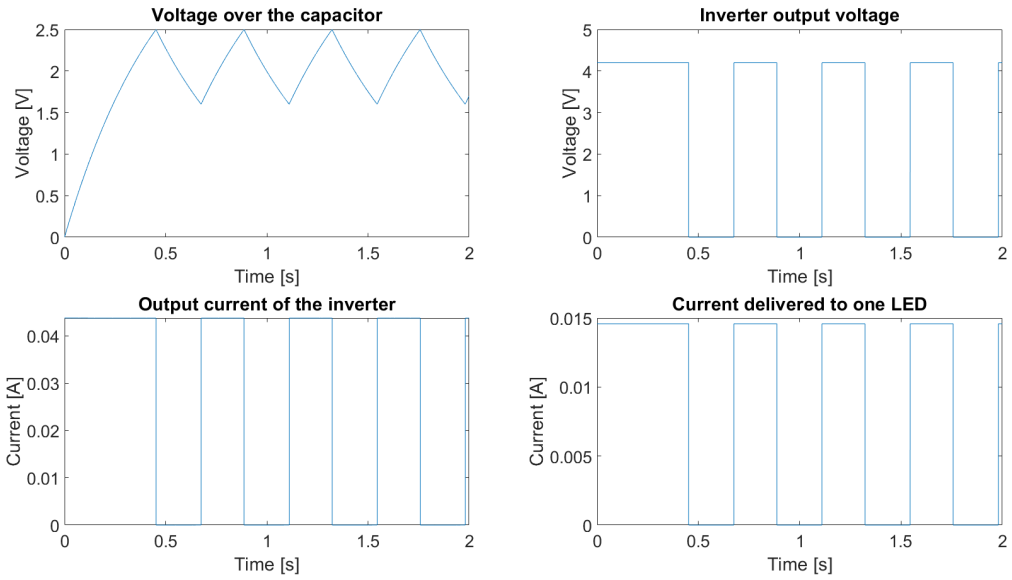

Figure A.2: Plots from the inverting Schmitt trigger model. Top left: The relation between the voltage over the capacitor and time. Top right: The relation between the output voltage of the inverter and the time. Bottom left: The relation between the output current of the inverter and the time. Bottom right: The relation between the current delivered to one LED and the time.

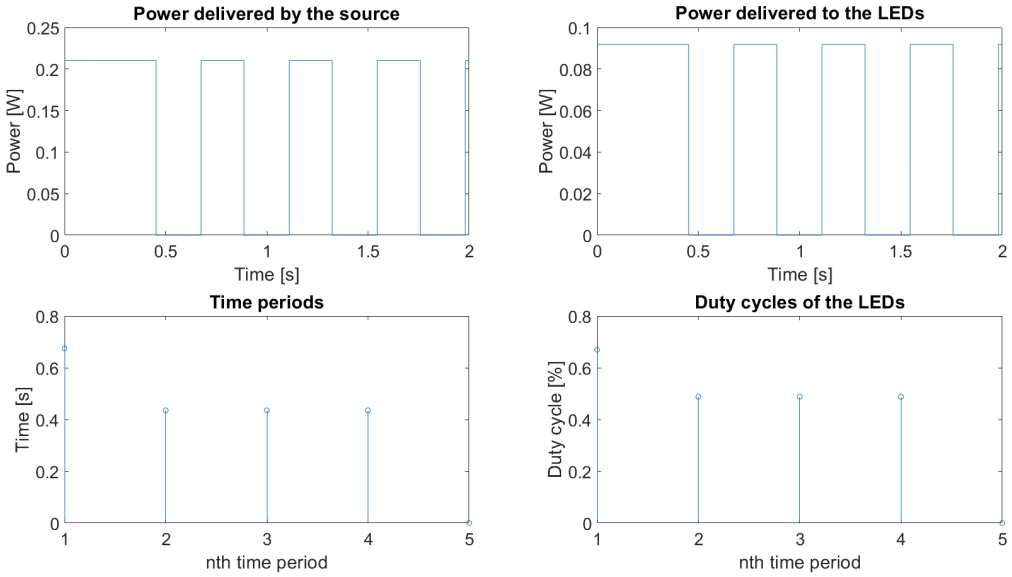

Figure A.3: Plots from the inverting Schmitt trigger model. Top left: The relation between power delivered by the source and time. Top right: The relation between the power delivered to the LEDs and the time. Bottom left: shows multiple cycles of the combined duration of one high and one low inverter output period. Bottom right: The duty cycles of the LEDs being operational.

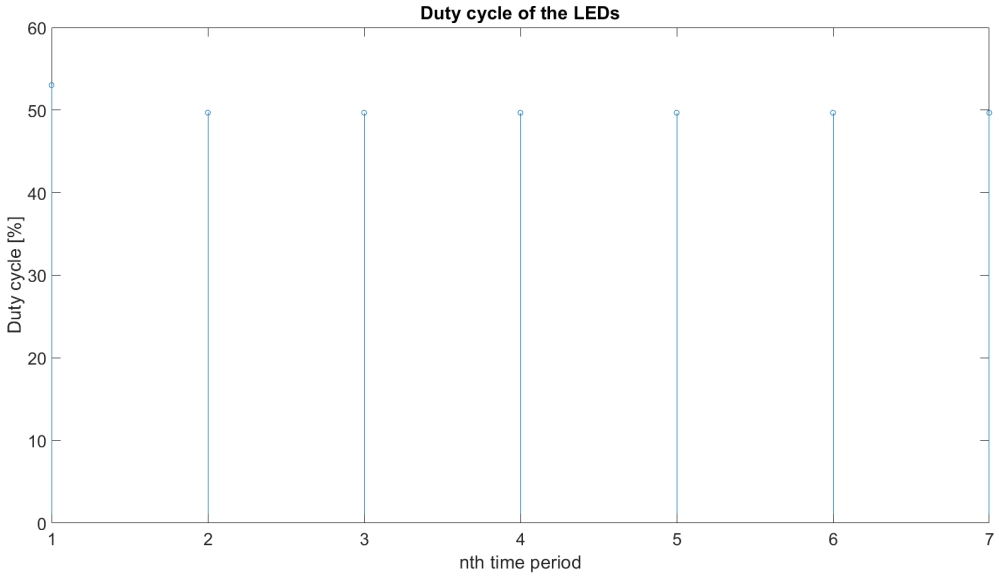

Figure A.4: Plot of the duty cycle of an LED from the chained inverting Schmitt trigger model.

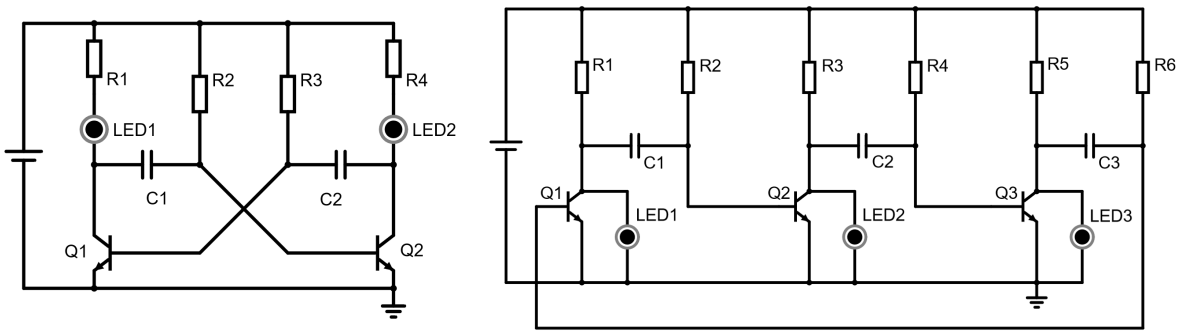

(a) LED series implementation.

(b) LED parallel implementation with third branch.

Figure A.5: Schematics of a bipolar junction transistor oscillator.

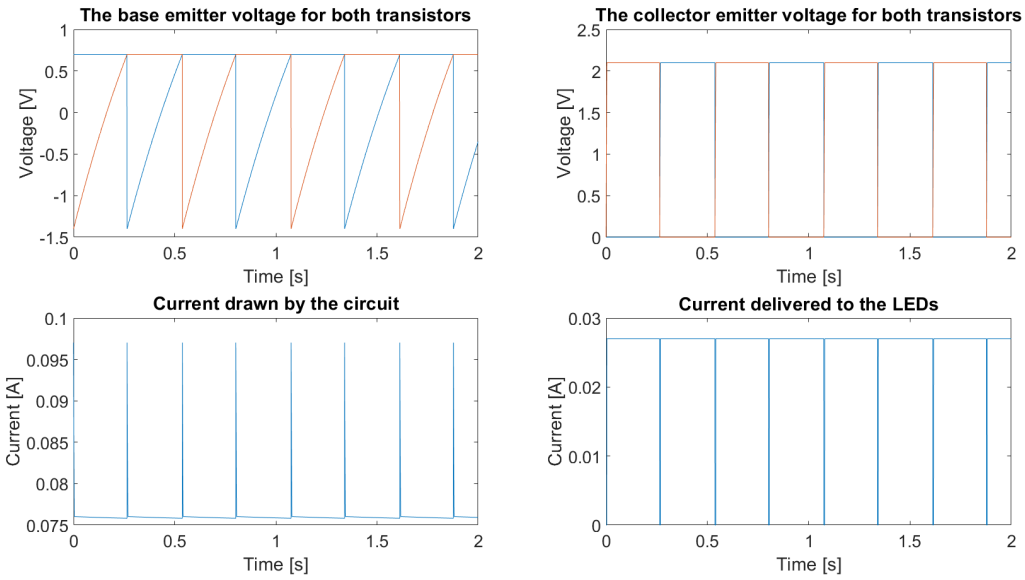

Figure A.6: Plots from the bipolar junction transistor model. Top left: The base emitter voltage of the transistors over time. Top right: The collector emitter voltage of the transistors over time. Bottom left: The current drawn from the source by the driver circuit. Bottom right: The combined current delivered to the LEDs.

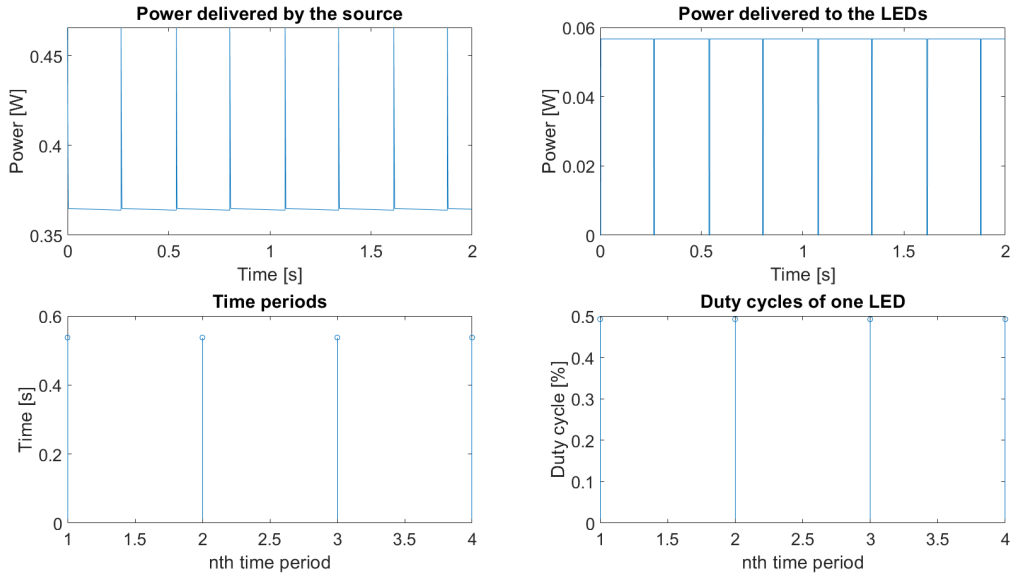

Figure A.7: Plots from the bipolar junction transistor model. Top left: The power delivered from the source to the circuit over time. Top right: The delivered to the LEDs over time. Bottom left: The duration of each time period. Bottom right: The duty cycle of one LED for each time period.

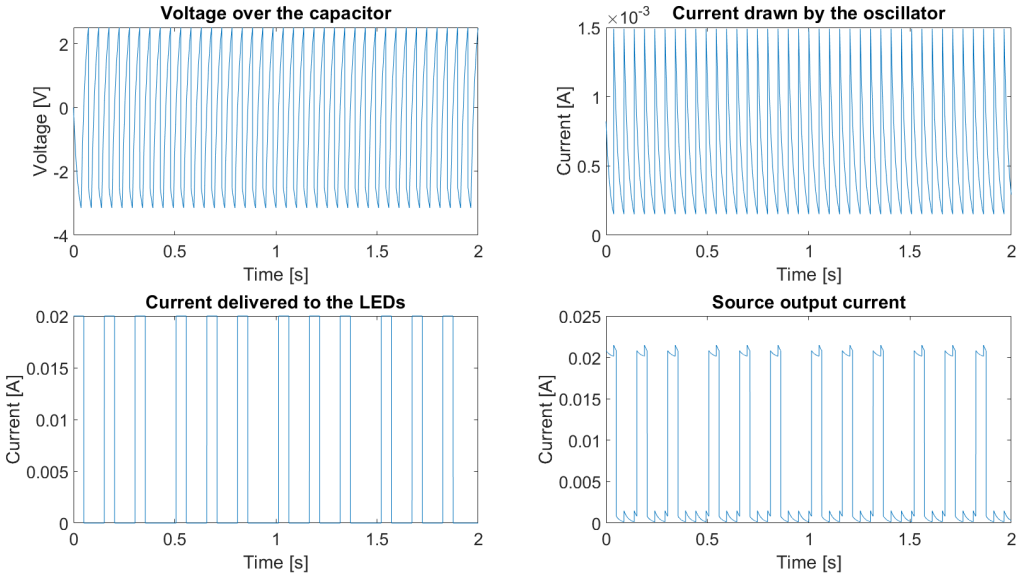

Figure A.8: Plots from the 4017 clocked decade counter model. Top left: The voltage over the capacitor $C1$ as a function of time. Top right: The current drawn by the oscillatory part of the circuit as a function of time. Bottom left: The current delivered to the LEDs as a function of time. Bottom right: shows current output of the source that is drawn by the entire circuit as a function of time.

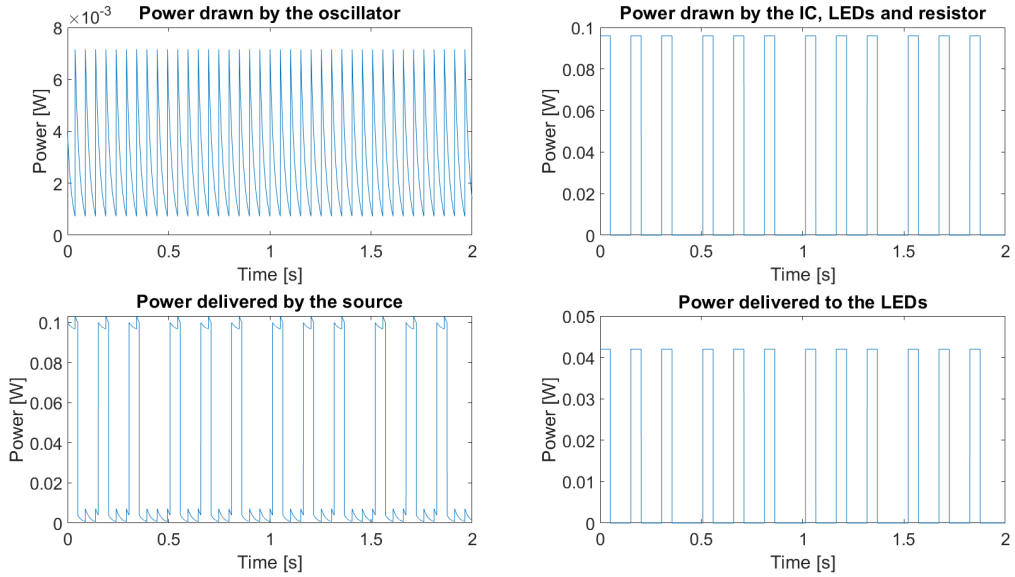

Figure A.9: Plots from the 4017 clocked decade counter model. Top left: The power used by the oscillatory circuit as a function of time. Top right: The power used by the IC, LED and resistor as a function of time. Bottom left: The power supplied by the source to the circuit as a function of time. Bottom right: The power delivered to the LEDs as a function of time.

Table A.1: LED driver circuit model parameters.

Circuit model	Bipolar junction transistor	Clocked decade counter	Inverting Schmitt trigger
Average power [W]	0.3651	0.0320	0.1164
Average LED power [W]	0.0559	0.0128	0.0509
LED power percentage [%]	15.3	39.91	43.74
Current per operational LED [A]	0.0270	0.0200	0.0146
Oscillation period [s]	0.5376	0.5065	0.4353
Combined LED duty cycle	100	30	49
Blinking type	2 LEDs alternating	3 LEDs alternating	3 LEDs simultaneously

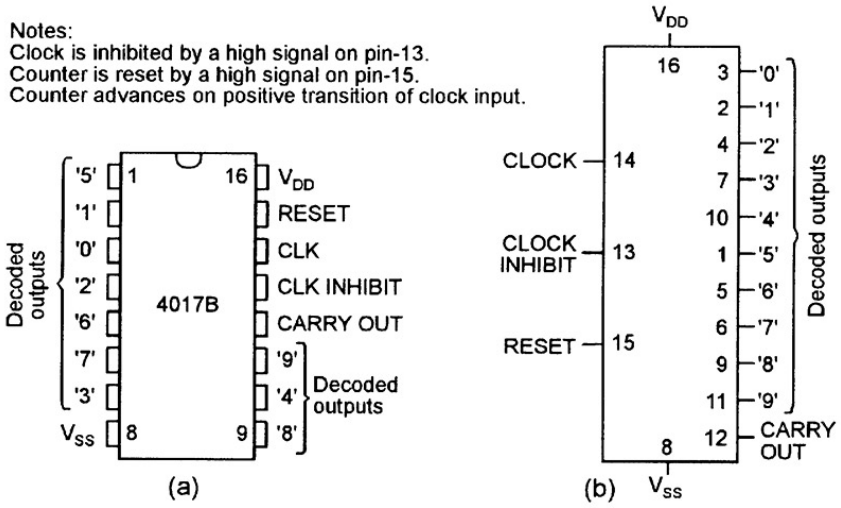

Figure A.10: Outline and pin designations (a) and basic functional diagram; (b) of the 4017B decade counter/divider IC (from [26]).

Table A.2: Specifications of viable LEDs for the product.

LED	Intensity (cd)			Angle (°)	power dissipation (mW)			Forward voltage (V)			Forward current (mA)			colour
artikelnr,	min	typical	max		max (sheet)	typical	max	min	typical	max	Typical	max	peak	
VLMY51Z1AA-GS08	4.5	7.1	9	120	530	308	530	1.9	2.2	2.65	140	200	1000	Yellow
LY G6SP-CADB-36-1	2.24		7.1	120	560	308	530	2.05	2.2	2.65	140	200	1000	Yellow
LA B6SP-CBEA-24-1	5.6		11.2	120		301	530	1.9	2.15	2.65	140	200	1000	Amber
LS B6SP-CADB-1-1	2.8		7.1	120		301	530	1.9	2.15	2.65	140	200	1000	Red
LA G6SP-DAFA-24-1	4.5		14	120		301	500	1.9	2.15	2.5	140	200	1000	Amber
LR G6SP-CBEA-1-1	3.55		9	120		294	500	1.9	2.1	2.5	140	200	1000	Red
GY DA SPA1,23FTGP-36-1	5		6	120		215	650	1.6	2.15	2.6	100	250		Yellow
GY DA SPA1,23FSFU-36-1	3.2		5.5	120		215	650	1.6	2.15	2.6	100	250		Yellow
LA G5AP-CZDZ-24-1	3.9		7.1	145		207	500	1.9	2.07	2.5	100	200	500	Amber
LTST-E680VEWT	1.12		4.5	120	150	125	150		2.5	3	50	50	100	Red
VLMY334BACB-GS08	1.8	2.3	4.5	120	200	115	196	1.9	2.3	2.8	50	70	100	Yellow
LAE67F-AABA-24-1-Z	1.12		2.24	120	190	115	185.5	2.05	2.3	2.65	50	70	100	Amber
VLMK334BACB-GS08	1.8	2.8	4.5	120	200	112.5	196	1.9	2.25	2.8	50	70	100	Amber
VLMK234ABCA-GS08	1.4	2.5	3.55	120	200	112.5	196	1.9	2.25	2.8	50	70		Amber
VLMR334BACB-GS08	1.8	2.2	4.5	120	200	110	196	1.9	2.2	2.8	50	70	100	Red
VLMR234ABCA-GS08	1.4	2	3.55	120	200	110	196	1.9	2.2	2.8	50	70		Red
VLMY234ABCA-GS08	1.4	2	3.55	120	200	110	196	1.9	2.2	2.8	50	70		Yellow
LA ETSF-BACB-24-1	1.8		4.5	120		107.5	185.5	1.9	2.15	2.65	50	70	100	Amber
LO E67F-BADA-24-1	1.8		5.6	120		107.5	175	1.9	2.15	2.5	50	70	100	Orange
LSE6SF-V2BA-1-1	0.9		2.24	120	190	107.5	175	1.9	2.15	2.5	50	70	100	Red
LO E6SF-ABCB-24-1	0.9		2.24	120		107.5	175	1.9	2.15	2.5	50	70	100	Orange
VLMK32ABBB-GS08	1.4		2.85	120	200	0	200	1.85		3.03	50	70		Amber
LO P47F-AABB-24-3A5A	1.12		2.8	120		67.5	127.5	1.8	2.25	2.55	30	50	100	Orange
LY P47F-V2BA-36-3B5B	0.9		2.24	120		61.5	135	1.95	2.05	2.7	30	50	100	Yellow
LA P47F-V2BB-24-3B5A	0.9		2.8	120		61.5	127.5	1.95	2.05	2.55	30	50	100	Amber
LS A67F-U2AB-1-3A4B	0.56		1.8	120		60	120	1.8	2	2.4	30	50	100	Red
KPHD-1608SECK-J4-PRV	1.2		2.46	120	84	44	84		2.2	2.8	20	30	150	Orange
ALMD-LG36-WZ002	1.38		2.9	100	120	42	120	1.8	2.1	2.4	20	50	100	Red
OVA-1088	1.4	2.7		90		42	78		2.1	2.6	20	30	100	Red

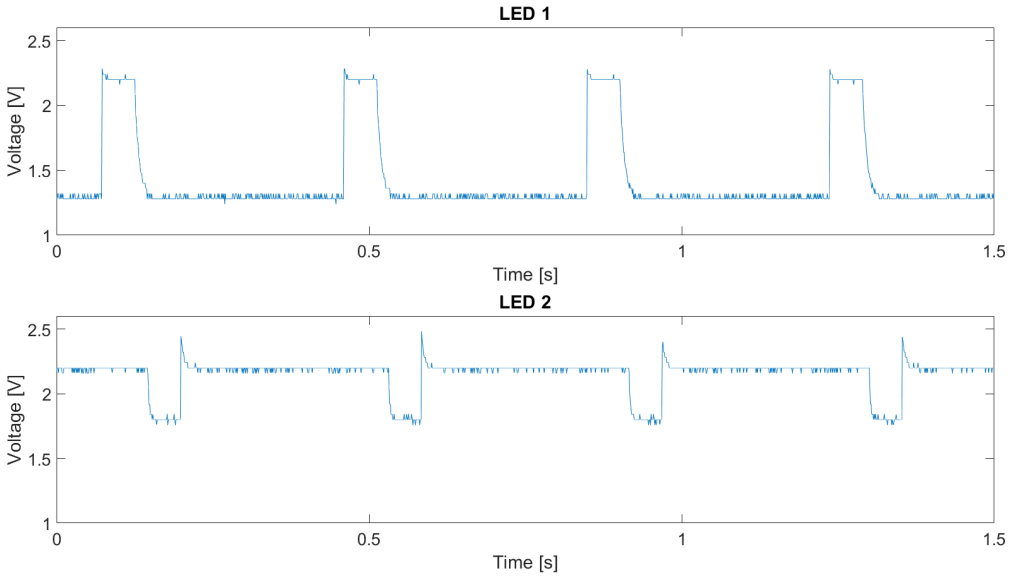

Figure A.11: Oscilloscope view of the voltage over both LEDs in the BJT oscillator.

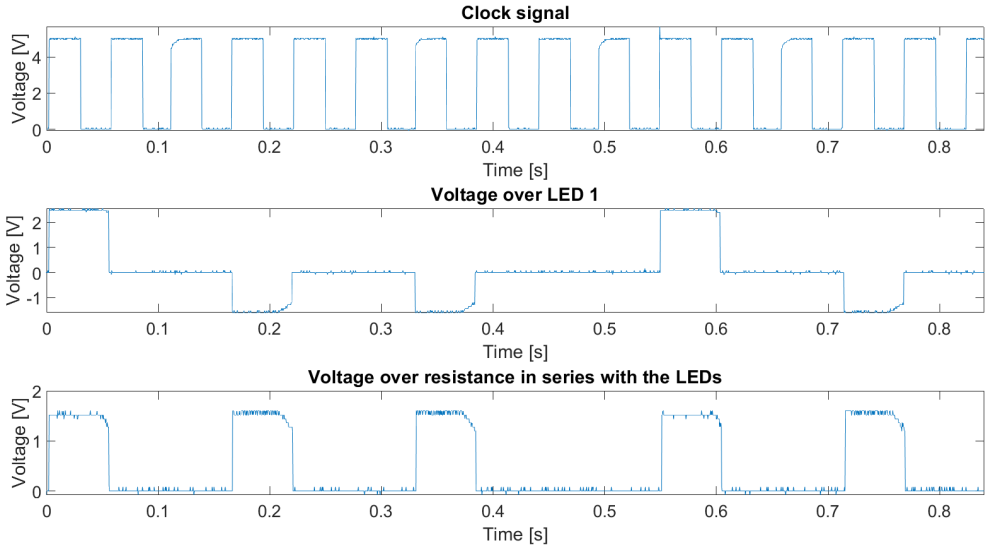

Figure A.12: Oscilloscope view of the voltage over different parts of the 4017 circuit.

Component	Specification	Number
Resistance	$100k\Omega$	1
Resistance	$4.7k\Omega$	1
Resistance	47Ω	1
Capacitance	$4.7\mu F$	1
NAND gate IC	Texas Instruments SN74AC00N	1
4017 IC	Texas Instruments CD74HC4017E	1
LED	LA G5AP-CZDZ-24-1	5

Table A.3: Components used in the final prototype.

Resistance [Ω]	Discharge time [s]	Peak current [mA]
99.2	68	17
82.4	60	20
68.4	58	23
56.1	55	23
46.9	55	29
38.6	51	29
33.2	48	33
27.1	47	35
22.0	46	36
14.9	43	43
12.3	43	39
10.2	42	39

Table A.4: Discharge times from 4.8 V to 2.0 V and peak currents with different resistances for a 0.1 F capacitor.

Appendix B

Collaboration

B.1 Dynamics

We kicked off the project with a meeting. In this meeting some base rules and intentions were drafted as to ensure a pleasant group experience. These included things like being on time, compensating for missed hours in leisure time and striving for attendance in the Tellegen Hall, where we had our own workspace, between $9:45$ and $17:30$. Afterwards a brainstorm session was held to determine the division of tasks, speculate on possible solutions for these tasks and drafting a general planning for the duration of the project (see table B.1).

Week	Scheduled activity
0	Make a group division
1	Literature research
2	Conclude the literature research and start with the design
3	Finalising design
4 + 5	Building and testing + Green-light assessment
6	Make a working prototype
7 + 8	Writing the thesis
9	Finishing the thesis + thesis deadline
10	Preparing the thesis defense
11	Thesis defense

The teamwork went pretty well; barely any miscommunications occurred, though informing other groups of important decisions or values did not always happen too quickly. Everyone was mostly kept up to speed due to our (almost) daily meetings. In general there is little to comment on the proceedings in our group.

B.2 Task division

The task of designing and implementing the battery free jogger light was split up in three different parts. These parts are energy harvesting, energy conversion and storage, lighting and casing. The energy harvesting group was tasked with delivering as much power as possible for small dimensions and weight. The energy conversion and storage group was tasked with converting the acquired signal from the energy harvesting group into something that can be stored and into something that powers the light source. The lighting and casing group was tasked with finding the most suitable light source and designing a suitable casing.
As the project progressed, the lighting and casing group was gradually lacking things to do as suitable LEDs were chosen and an initial design was made. The design could not be optimised as long as no specific dimensions of other components were known. The energy conversion and storage group on the other hand, had a considerable work load. It was therefore decided, that the lighting and casing group would take over the task of designing a circuit that would drive

the LEDs.
As the lighting and casing group was considering all the possible options for powering the LEDs, the energy conversion and storage group were starting to lack things to do. They required the LED driving circuit for further testing. Therefore, did the lighting and casing group start implementing and modelling in parallel as to speed up the process.

Appendix C

Models

C.1 Parameter definition

The parameters used in the models of the following section are defined as follows:

- V_O = the output voltage of a device represented as a voltage source
- V_I = the input voltage of a device
- V_{DD} = the source voltage
- V_F = the forward voltage of an LED
- V_T = a threshold voltage of a device, with + and - representing from low to high and high to low respectively
- V_C = the voltage over a capacitor, with $V_C(0)$ denoting the voltage over the transistor just before a state change was made at time $t = 0$
- V_{ce} = the voltage over the collector and emitter of a bipolar junction transistor
- V_{be} = the voltage over the base and emitter of a bipolar junction transistor
- V_{clk} = a voltage based clock signal
- I_O = the current output by the device that acts as a source
- I_{LED} = the current flowing through an LED
- P_I = the power delivered to the entire circuit by the source
- P_{LED} = the power delivered to the LED
- R = the resistance of a resistor
- C = the capacitance of a capacitor
- t = the time, with $t = 0$ always being the initial time of the new state after switching
- t_s = the time at which the circuit switches from state
- t_l = the time an LED starts conducting

A number is added to the subscript whenever more of the same parameter are present.

C.2 Inverting Schmitt trigger model

The model treats the inverting Schmitt trigger as either a voltage source or ground depending on the input voltage. Two different states are therefore defined, high output state (state 1) and low output state (state 2). For each state an equivalent circuit was determined and analysed. The time period T of one square wave is determined by adding up the switching times of both states. The duty cycle is determined by dividing the time in which the LEDs are operational by T. The average power is determined by summing P_I and averaging it over time. In the same way the average power supplied to the LEDs is determined. The power delivered to the LEDs as percentage of the total power is determined by dividing the average LED power by the average power.

C.2.1 State 1

In Figure C.1, the equivalent circuit of state 1 is shown.

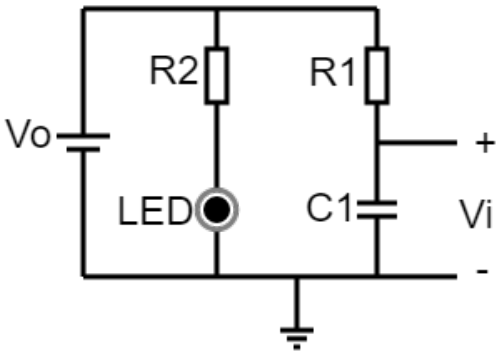

Figure C.1: Equivalent circuit of state 1 of the inverting Schmitt trigger oscillator.

This equivalent circuit is applicable if the following conditions are met:

- $V_O \geq V_F$
- $V_I \leq V_{T+}$

The relations within this circuit are expressed with the following equations:

$$V_I(t) = V_O - (V_O - V_C(0))e^{-\frac{t}{R_1 C_1}} \tag{C.1}$$

$$t_s = -R_1 C_1 \ln \frac{V_O - V_{T+}}{V_O - V_C(0)} \tag{C.2}$$

$$V_C(t) = V_I(t) \tag{C.3}$$

$$I_{LED} = \frac{V_O - V_F}{R_2} \tag{C.4}$$

$$I_O(t) = \frac{V_O - V_I}{R_1} + \frac{V_O - V_F}{R_2} \tag{C.5}$$

$$P_I(t) = V_{DD} I_O \tag{C.6}$$

$$P_{LED} = I_{LED} V_F \tag{C.7}$$

C.2.2 State 2

In Figure C.2, the equivalent circuit of state 2 is shown.

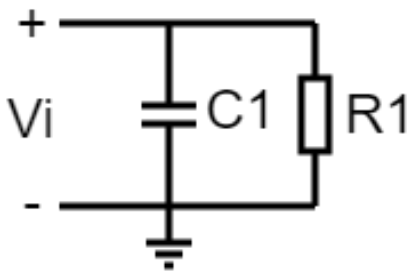

Figure C.2: Equivalent circuit of state 2 of the inverting Schmitt trigger oscillator.

This equivalent circuit is applicable if the following conditions are met:

- $V_I \geq V_{T-}$

The relations within this circuit are expressed with the following equations:

$$V_I(t) = V_C(0) e^{-\frac{t}{R_1 C_1}} \tag{C.8}$$

$$t_s = -R_1 C_1 \ln \frac{V_{T-}}{V_C(0)} \tag{C.9}$$

$$V_C(t) = V_I(t) \tag{C.10}$$

$$I_O = -\frac{V_C(0)}{R_1} e^{-\frac{t}{R_1 C_1}} \tag{C.11}$$

$$I_{LED} = 0 \tag{C.12}$$

$$P_I = 0 \tag{C.13}$$

$$P_{LED} = 0 \tag{C.14}$$

C.3 BJT oscillator circuit model

The BJT oscillator circuit model is based on the schematic in Figure 3.6 with the addition of two LEDs, both located parallel with the transistors similarly to the LEDs in Figure A.5b. The model treats the circuit to always be in one of two states. Each state corresponds to either $Q1$ conducting and $Q2$ turned off (state 1), or $Q1$ turned off and $Q2$ conducting (state 2). The duty cycle is determined by dividing the time in which the LEDs are operational by T. The average power is determined by summing P_I and averaging it over time. In the same way the average power supplied to the LEDs is determined. The power delivered to the LEDs as percentage of the total power is determined by dividing the average LED power by the average power.

C.3.1 State 1

State 1 is applicable if the following conditions are met:

- $V_{be1} = V_T$
- $V_{be2} \leq V_T$

The relations within the circuit at this state are expressed with the following equations:

$$V_{ce1} = 0 \tag{C.15}$$

$$t_l = -R_4 C_2 \ln \frac{V_F - V_{DD}}{V_{ce2}(0) - V_{DD}} \tag{C.16}$$

$$V_{ce2}(t) = \begin{cases} (V_{ce2}(0) - V_{DD}) e^{-\frac{t}{R_4 C_2}} + V_{DD}, & \text{if } t < t_l \\ V_F, & \text{if } t \geq t_l \end{cases} \tag{C.17}$$

$$V_{be2}(t) = (V_T - V_{DD} - V_{ce1}(0)) e^{-\frac{t}{R_2 C_1}} + V_{DD} \tag{C.18}$$

$$t_s = -R_2 C_1 \ln \frac{V_T - V_{DD}}{V_T - V_{DD} - V_{ce1}(0)} \tag{C.19}$$

$$I_{LED} = \begin{cases} 0, & \text{if } t < t_l \\ \frac{V_{DD} - V_F}{R_4}, & \text{if } t \geq t_l \end{cases} \tag{C.20}$$

$$P_{LED} = I_{LED} V_F \tag{C.21}$$

$$I_O(t) = \frac{V_{DD} - V_{ce1}}{R_1} + \frac{V_{DD} - V_{be2}}{R_2} + \frac{V_{DD} - V_{be1}}{R_3} + \frac{V_{DD} - V_{ce2}}{R_4} \tag{C.22}$$

$$P_I(t) = V_{DD} I_O(t) \tag{C.23}$$

C.3.2 State 2

State 2 is applicable if the following conditions are met:

- $V_{be1} \leq V_T$
- $V_{be2} = V_T$

The relations within the circuit at this state are expressed with the following equations:

$$V_{ce1}(t) = \begin{cases} (V_{ce1}(0) - V_{DD})e^{-\frac{t}{R_1 C_1}} + V_{DD}, & \text{if } t < t_l \\ V_F, & \text{if } t \geq t_l \end{cases} \tag{C.24}$$

$$t_l = -R_1 C_1 \ln \frac{V_F - V_{DD}}{V_{ce1}(0) - V_{DD}} \tag{C.25}$$

$$V_{ce2} = 0 \tag{C.26}$$

$$V_{be1}(t) = (V_T - V_{DD} - V_{ce2}(0))e^{-\frac{t}{R_3 C_2}} + V_{DD} \tag{C.27}$$

$$t_s = -R_3 C_2 \ln \frac{V_T - V_{DD}}{V_T - V_{DD} - V_{ce2}(0)} \tag{C.28}$$

$$I_{LED} = \begin{cases} 0, & \text{if } t < t_l \\ \frac{V_{DD} - V_F}{R_1}, & \text{if } t \geq t_l \end{cases} \tag{C.29}$$

$$P_{LED} = I_{LED} V_F \tag{C.30}$$

$$I_O(t) = \frac{V_{DD} - V_{ce1}}{R_1} + \frac{V_{DD} - V_{be2}}{R_2} + \frac{V_{DD} - V_{be1}}{R_3} + \frac{V_{DD} - V_{ce2}}{R_4} \tag{C.31}$$

$$P_I(t) = V_{DD} I_O(t) \tag{C.32}$$

C.4 Clocked decade counter circuit model

The model of the clocked decade counter circuit seperatly analyses the NAND oscillator and the clocked decade counter. The NAND oscillator is further broken down into two states; in state 1 the output of NAND $U1:A$ is high and the output of $U1:B$ is low, while in state 2 the output of $U1:A$ is low and the output of $U1:B$ is high. Equivalent circuit have been modelled for both states, treating the NAND as either a voltage source or gound depending on the output. The clocked decade part of the circuit is represented by a single equivalent circuit that is applicable whenever an LED is connected to the output that is high. In that case, the IC is treated as a voltage source. The capacitor is assumed to be uncharged at time $t = 0$. The duty cycle is determined by dividing the time in which the LEDs are operational by T. The average power is determined by summing P_I and averaging it over time. In the same way the average power supplied to the LEDs is determined. The power delivered to the LEDs as percentage of the total power is determined by dividing the average LED power by the average power.

C.4.1 State 1

The equivalent NAND circuit of state 1 is shown in Figure C.3.

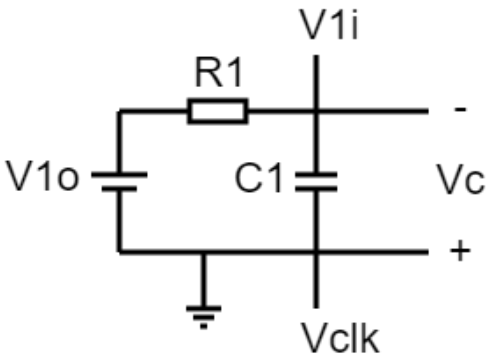

Figure C.3: Equivalent circuit of state 1 of the NAND oscillator.

State 1 is applicable under the following conditions:

- $V_{I1} \leq V_{T+}$
- $V_{I2} \geq V_{T-}$

The relations of the NAND oscillator circuit in state 1 can be expressed as:

$$V_{clk} = 0 \tag{C.33}$$

$$V_{1I} = V_{1O} + (V_C(0) - V_{1O})e^{-\frac{t}{R_1 C_1}} \tag{C.34}$$

$$t_s = -R_1 C_1 \ln \frac{V_{T+} - V_{1O}}{V_C(0) - V_{1O}} \tag{C.35}$$

$$V_C = -V_{1I} \tag{C.36}$$

$$I_O = \frac{V_{1O} - V_{1I}}{R_1} \tag{C.37}$$

$$P_I = I_O V_{DD} \tag{C.38}$$

C.4.2 State 2

The equivalent NAND circuit of state 2 is shown in Figure C.4.

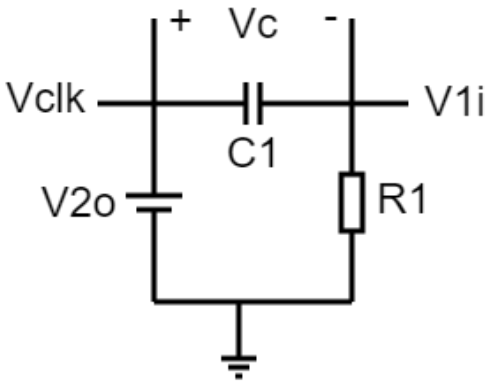

Figure C.4: Equivalent circuit of state 2 of the NAND oscillator.

State 2 is applicable under the following conditions:

- $V_{I2} \leq V_{T+}$
- $V_{I1} \geq V_{T-}$

The relations of the NAND oscillator circuit in state 2 can be expressed as:

$$V_{clk} = V_{2O} \tag{C.39}$$

$$V_{1I} = (V_{1O} - V_C(0))e^{-\frac{t}{R_1 C_1}} \tag{C.40}$$

$$t_s = -R_1 C_1 \ln \frac{V_{T-}}{V_{1O} - V_C(0)} \tag{C.41}$$

$$V_C = V_{1O} - V_{1I} \tag{C.42}$$

$$I_O = \frac{V_{1I}}{R_1} \tag{C.43}$$

$$P_I = I_O V_{DD} \tag{C.44}$$

C.4.3 LED equivalent circuit

The equivalent circuit of the IC when an LED is connected to the output that is high, is shown in Figure C.5.

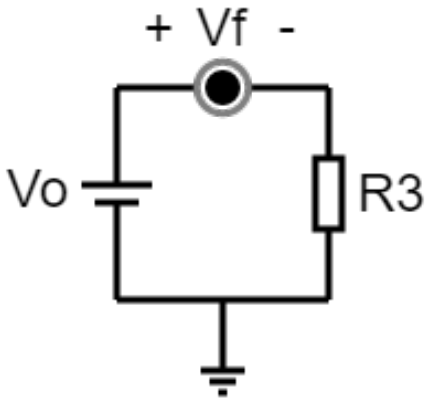

Figure C.5: Equivalent circuit of the clocked decade counter with LED on high output pin.

This equivalent circuit is applicable if the following condition is met:

- $V_O \geq V_F$

The relations of this equivalent circuit can be expressed as:

$$I_{LED} = \frac{V_O - V_F}{R_3} \tag{C.45}$$

$$P_{LED} = I_{LED} V_F \tag{C.46}$$

$$P_I = I_{LED} V_{DD} \tag{C.47}$$

Appendix D

MATLAB codes

D.1 Inverting Schmitt trigger model

```
%insert parameters
Vdd = 4.8;      %source voltage supplied to the inverting schmitt
    trigger
Vf = 2.1;       %forward voltage of the LED
VTup=2.5;       %voltage threshold for the inverting schmitt trigger
    for the input voltage going from low to high
VTdown=1.6;     %voltage threshold for the inverting schmitt trigger
    for the output voltage going from high to low
R1 = 10^5;       %Resistance of the resistor located between the in/
    output of the schmitt trigger
C1 = 5*10^-6;      %capacitance of the capacitor located between the
    input of the inverter and ground
R2 = 144;     %resistance of the resistor that's in series with the
    LED
N = 100;       %number of switch cycles
S=10000;
Voh=4.2;
Vc=0;
Tcalc=1;
Tmax=2;
state=1;
t=0;
Ptot=[];
PledM=[];
tsw=[];
IledM=[];
IoutM=[];
VcM=[];
VcT=[];
StateRec=[1];
n=1;
t_EndFlag=0;

while t_EndFlag==0
                [K,tnew,Vc,Vcfull,Pin,Pled,Iout,Iled,state]=
                    schmitt_model(Tcalc,S,R1,R2,C1,Vc,Vdd,Vf,VTup,VTdown,
                    Voh,state,1);
                if n==1
```

```
31                      t=[t(1:round(K/Tcalc*t(end))-1),tnew+t(end)];
32                      n=0;
33                  else
34                      t=[t,tnew+t(end)];
35                  end
36                  StateRec=[StateRec,state];
37                  Ptot=[Ptot,Pin];
38                  PledM=[PledM,Pled];
39                  tsw=[tsw,tnew(end)];
40                  IledM=[IledM,Iled];
41                  IoutM=[IoutM,Iout];
42                  VcM=[VcM,Vc];
43                  VcT=[VcT,Vcfull];
44                  if t(end) > Tmax
45                      t_EndFlag=1;
46                      t=t(1:Tmax.*S);
47                      Ptot=Ptot(1:Tmax.*S);
48                      IoutM=IoutM(1:Tmax.*S);
49                      VcT=VcT(1:Tmax.*S);
50                  end
51  end
52
53  b=0;
54  T=zeros(1,round(length(tsw)./2));
55  d=zeros(1,round(length(tsw)./2));
56  for q=1:(length(tsw)/2)
57      for a=1:2
58          T(q)=T(q)+tsw(a+b);
59          if a==2
60              d(q)=tsw(a+b-1)./T(q);
61          end
62      end
63      b=b+2;
64  end
65
66  PledT=[];
67  IledT=[];
68  TT=[];
69  dT=[];
70  Vout=[];
71
72  for q=1:length(tsw)
73      tlength = ones(1,round(tsw(q).*S));
74      PledT = [PledT, PledM(q).*tlength];
75      IledT = [IledT, IledM(q).*tlength];
76      if StateRec(q)==1
77          Vout = [Vout, Voh.*tlength];
78      else
```

```
79          Vout = [Vout, 0.*tlength];
80      end
81  end
82
83  PledT=PledT(1:S.*Tmax);
84  IledT=IledT(1:S.*Tmax);
85  Vout=Vout(1:S.*Tmax);
86
87  Pave = sum(Ptot)/length(Ptot);
88  Pledave = sum(PledT)./length(PledT);
89  PledFrac = Pledave./Pave;
90
91  figure
92  subplot(2,2,1)
93  plot(t,Ptot)
94  title('Power delivered by the source')
95  xlabel('Time [s]')
96  ylabel('Power [W]')
97  set(gca,'fontsize',20);
98
99  subplot(2,2,2)
100 plot(t,PledT)
101 title('Power delivered to the LEDs')
102 xlabel('Time [s]')
103 ylabel('Power [W]')
104 set(gca,'fontsize',20);
105
106 subplot(2,2,3)
107 stem(T)
108 title('Time periods')
109 xlabel('nth time period')
110 ylabel('Time [s]')
111 set(gca,'fontsize',20);
112
113 subplot(2,2,4)
114 stem(d)
115 title('Duty cycles of the LEDs')
116 xlabel('nth time period')
117 ylabel('Duty cycle [%]')
118 set(gca,'fontsize',20);
119
120 figure
121 subplot(2,2,1)
122 plot(t,VcT)
123 title('Voltage over the capacitor')
124 xlabel('Time [s]')
125 ylabel('Voltage [V]')
126 set(gca, 'fontsize',20);
```

```
127
128 subplot(2,2,2)
129 plot(t,Vout)
130 title('Inverter output voltage')
131 xlabel('Time [s]')
132 ylabel('Voltage [V]')
133 set(gca,'fontsize',20);
134
135 subplot(2,2,3)
136 plot(t,IoutM)
137 title('Output current of the inverter')
138 xlabel('Time [s]')
139 ylabel('Current [A]')
140 set(gca,'fontsize',20);
141
142 subplot(2,2,4)
143 plot(t,IledT)
144 title('Current delivered to one LED')
145 xlabel('Time [s]')
146 ylabel('Current [A]')
147 set(gca,'fontsize',20);
```

```
1  function [ILED, Iin, PLED, Pin, Vc, StateOut, td]=InverterBlock(t,
       NSample, R, RLED, C, Vout, Vf, Vdd, VT, Vm, StateIn, Type)
2      switch Type
3          case 1                                  %LED inverter block
4              if StateIn==1
5                  ILED = (Vout-Vf)/RLED;
6                  StateOut = 0;
7              else
8                  ILED=0;
9                  StateOut=1;
10             end
11             Iin=ones(1,NSample).*ILED;
12             PLED=ILED.*Vf;
13             Pin = Iin*Vdd;
14             Vc = zeros(1,NSample);
15             td=t(2);
16         case 2
17             if StateIn == 1
18                 ILED = (Vout-Vf)/RLED;
19                 Iin = ILED + (Vout-Vm)./R.*exp(-t/(R.*C));
20                 Pin = Iin.*Vdd;
21                 StateOut=0;
22                 td = -R.*C.*log((Vout-VT(1))/(Vout-Vm));
23                 Vc = Vout-(Vout-Vm).*exp(-t/(R.*C));
24             else
25                 ILED=0;
26                 Iin=-Vm./R.*exp(-t./(R.*C));
```

```
27                  Pin=zeros(1,NSample);
28                  StateOut=1;
29                  td = -R.*C.*log(VT(2)/Vm);
30                  Vc= Vm.*exp(-t/(R.*C));
31              end
32              PLED=ILED.*Vf;
33
34          case 3
35              if StateIn == 1
36                  Iin = (Vout-Vm)./R.*exp(-t./(R.*C));
37                  Pin = Vdd.*Iin;
38                  StateOut = 0;
39                  td = -R.*C.*log((Vout-VT(1))./(Vout-Vm));
40                  Vc = Vout-(Vout-Vm).*exp(-t./(R.*C));
41              else
42                  Iin = -Vm./R.*exp(-t./(R.*C));
43                  Pin=zeros(1,NSample);
44                  StateOut=1;
45                  td = -R.*C.*log(VT(2)./Vm);
46                  Vc = Vm.*exp(-t./(R.*C));
47              end
48              ILED = 0;
49              PLED = 0;
50      end
51      if td == -inf
52          td=0;
53      else
54      end
55  end
```

D.2 BJT model

```
1
2  %insert parameters
3  Vdd = 4.8;          %source voltage
4  Vf = 2.1;           %forward voltage of the LED
5  VT=0.7;
6  R2 = 10*10^3;
7  R3 = 10*10^3;
8  C1= 64*10^(-6);
9  C2 = 66*10^(-6);
10 R1 = 100;
11 R4 = 100;
12 Nled = 2;
13 Tmax=2;
14 t=0;
15 Vc1m=Vf;
16 Vc2m=0;
```

```
17 Vc1=0;
18 Vc2=0;
19 state=1;
20 tl=[];
21 ts=[];
22 IinM=[];
23 IledM=[];
24 Vbe1M=[];
25 Vbe2M=[];
26 PledM=[];
27 Ptot=[];
28 Vc1M=[];
29 Vc2M=[];
30 StateRec=[];
31
32 % Time frame and corresponding step size in s
33 L=1;
34 N=100000;
35 tcalc=linspace(0,L,N);
36
37 t_EndFlag=0;
38 start=1;
39
40 while t_EndFlag==0
41     [Iin,Iled,Vbe1,Vbe2,tsnew,tlnew,Pled,Pin,Vc1,Vc2,state] =
          AstableMultivibrator(tcalc,L,Vdd,Vf,VT,R1,R2,R3,R4,C1,C2,state
          ,Vc1m,Vc2m,N);
42     Vc1m=Vc1(end);
43     Vc2m=Vc2(end);
44     if start==1
45         t=[t(1:round(N.*t(end))-1),tsnew+t(end)];
46         start=0;
47     else
48         t=[t,tsnew+t(end)];
49     end
50     IinM=[IinM,Iin];
51     IledM=[IledM,Iled];
52     Vbe1M=[Vbe1M,Vbe1];
53     Vbe2M=[Vbe2M,Vbe2];
54     ts=[ts,tsnew(end)];
55     tl=[tl,tlnew];
56     Vc1M=[Vc1M,Vc1];
57     Vc2M=[Vc2M,Vc2];
58     StateRec=[StateRec,state];
59     Ptot=[Ptot,Pin];
60     PledM=[PledM,Pled];
61     if t(end) > Tmax
62         t_EndFlag=1;
```

```
63            t=t(1:Tmax*N);
64            IinM=IinM(1:Tmax*N);
65            IledM=IledM(1:Tmax*N);
66            Vbe1M=Vbe1M(1:Tmax*N);
67            Vbe2M=Vbe2M(1:Tmax*N);
68            Vc1M=Vc1M(1:Tmax*N);
69            Vc2M=Vc2M(1:Tmax*N);
70            Ptot=Ptot(1:Tmax*N);
71            PledM=PledM(1:Tmax*N);
72        end
73    end
74
75    b=0;
76    T=zeros(1,round(length(ts)./2));
77    d=zeros(1,round(length(ts)./2));
78    for q=1:(length(ts)/2)
79        for a=1:2
80            T(q)=T(q)+ts(a+b);
81            if a==2
82                d(q)=ts(a+b-1)./T(q);
83            end
84        end
85        b=b+2;
86    end
87
88    Pave = sum(Ptot)/length(Ptot);
89    Pledave = sum(PledM)./length(PledM);
90    PledFrac = Pledave./Pave;
91
92    figure
93    subplot(2,2,1)
94    plot(t,Ptot)
95    title('Power delivered by the source')
96    xlabel('Time [s]')
97    ylabel('Power [W]')
98    set(gca,'fontsize',20);
99
100   subplot(2,2,2)
101   plot(t,PledM)
102   title('Power delivered to the LEDs')
103   xlabel('Time [s]')
104   ylabel('Power [W]')
105   set(gca,'fontsize',20);
106
107   subplot(2,2,3)
108   stem(T)
109   title('Time periods')
110   xlabel('nth time period')
```

```
111 ylabel('Time [s]')
112 set(gca,'fontsize',20);
113
114 subplot(2,2,4)
115 stem(d)
116 title('Duty cycles of one LED')
117 xlabel('nth time period')
118 ylabel('Duty cycle [%]')
119 set(gca,'fontsize',20);
120
121 figure
122 subplot(2,2,1)
123 plot(t,Vbe1M)
124 hold on
125 plot(t,Vbe2M)
126 title('The base emitter voltage for both transistors')
127 xlabel('Time [s]')
128 ylabel('Voltage [V]')
129 set(gca,'fontsize',20);
130
131 subplot(2,2,2)
132 plot(t,Vc1M)
133 hold on
134 plot(t,Vc2M)
135 title('The collector emitter voltage for both transistors')
136 xlabel('Time [s]')
137 ylabel('Voltage [V]')
138 set(gca,'fontsize',20);
139
140 subplot(2,2,3)
141 plot(t,IinM)
142 title('Current drawn by the circuit')
143 xlabel('Time [s]')
144 ylabel('Current [A]')
145 set(gca,'fontsize',20);
146
147 subplot(2,2,4)
148 plot(t,IledM)
149 title('Current delivered to the LEDs')
150 xlabel('Time [s]')
151 ylabel('Current [A]')
152 set(gca,'fontsize',20);
```

```
1
2 function [Iin,Iled,Vbe1,Vbe2,ts,tl,Pled,Pin,Vc1,Vc2,StateOut] =
    AstableMultivibrator(t,T,Vdd,Vf,VT,R1,R2,R3,R4,C1,C2,state,Vc1m,
    Vc2m,S)
3
4 if(state == 1)
```

```
%------------------------State 1 (TR1 ON, TR2 OFF) Description
    ------------------
%Vce1
Vc1=zeros(1,S.*T);

%Vce2
Vc2=(Vc2m-Vdd).*exp(-t./(R4.*C2))+Vdd;

tl=-R4.*C2.*log((Vf-Vdd)./(Vc2m-Vdd));

Vc2(round(S.*tl):end)=Vf;

%Vbe1
Vbe1 =VT.*ones(1,S.*T);

%Vbe2
Vbe2=(VT-Vdd-Vc1m).*exp(-t./(R2.*C1))+Vdd;

%time till switch t
ts=-R2.*C1.*log((VT-Vdd)./(VT-Vdd-Vc1m));

%Pled
Iled= zeros(1,S.*T);
Iled(round(S.*tl):end)=(Vdd-Vf)./R4;
Pled=Iled.*Vf;

StateOut=2;

%-------------------------------------------------------------------------------
elseif(state ==2)
%------------------------State 2 (TR1 OFF, TR2 ON) Description
    ------------
%Vce1
Vc1=(Vc1m-Vdd).*exp(-t./(R1.*C1))+Vdd;

tl=-R1.*C1.*log((Vf-Vdd)./(Vc1m-Vdd));

Vc1(round(S.*tl):end)=Vf;

%Vce2
Vc2=zeros(1,S.*T);

%Vbe1
Vbe1=(VT-Vdd-Vc2m).*exp(-t./(R3.*C2))+Vdd;

%Vbe2
Vbe2=VT.*ones(1,S.*T);

```

```
%time till switch t
ts=-R3.*C2.*log((VT-Vdd)./(VT-Vdd-Vc2m));

%Pled
Iled= zeros(1,S.*T);
Iled(round(S.*tl):end)=(Vdd-Vf)./R1;
Pled=Iled.*Vf;

StateOut=1;
%-------------------------------------------------------------------------
else
end
%input power
Iin=(Vdd-Vc1)./R1+(Vdd-Vbe2)./R2+(Vdd-Vbe1)./R3+(Vdd-Vc2)./R4;
Pin=Vdd.*Iin;

Iin=Iin(1:round(ts.*S));
Iled=Iled(1:round(ts.*S));
Vbe1=Vbe1(1:round(ts.*S));
Vbe2=Vbe2(1:round(ts.*S));
Pled=Pled(1:round(ts.*S));
Pin=Pin(1:round(ts.*S));
Vc1=Vc1(1:round(ts.*S));
Vc2=Vc2(1:round(ts.*S));
ts=t(1:round(ts.*S));
return
```

D.3 4017 IC model

```
%Define specs
R2=4.7.*10^3;
C1=4.7*10^-6;
VOH_NAND = 3.86;
VIH_NAND = 3.15;
VIL_NAND = 1.35;
VOH_CLKDIV = 4.7;
Vf=2.1;
RLED =130;
Vcc=4.8;
T = 2;                                  %total Time period of
    modelling [s]
SperS = 10000;                          %samples per second
NSample = T.*SperS;                     %total number of samples
t=linspace(0,T,NSample);
State=1;
Vcm=0;
LEDS=3;
LEDposition=[1, 0, 0, 1, 0, 0, 1, 0, 0, 0];
```

```
19 t_endflag=0;
20 indextracker=0;
21 td=zeros(1,400);
22 Vclk=zeros(1,400);
23 Iin_NAND_T=zeros(1,NSample);
24 Iin_NAND=zeros(1,NSample);
25 Pin_NAND_T=zeros(1,NSample);
26 Pin_NAND=zeros(1,NSample);
27 Vc_T=zeros(1,NSample);
28 Vc=zeros(1,NSample);
29 counter=0;
30
31 i=1;
32 while t_endflag~=1
33 [Vclk(i),td(i),Iin_NAND_T,Pin_NAND_T,Vc_T,State]=NANDoscillator(State
      ,R2,C1,VIH_NAND,VIL_NAND,VOH_NAND,Vcm,Vcc,t);
34 tSample=round(td(i).*NSample./T);
35 Iin_NAND(indextracker+1:indextracker+tSample)=Iin_NAND_T(1:tSample);
36 Pin_NAND(indextracker+1:indextracker+tSample)=Pin_NAND_T(1:tSample);
37 Vcm=Vc_T(tSample);
38 Vc(indextracker+1:indextracker+tSample)=Vc_T(1:tSample);
39 i=i+1;
40 indextracker=indextracker+tSample;
41 if sum(td)>=T
42     t_endflag=1;
43 end
44 end
45
46 [~,tfit]=min(td);
47 td=td(1:tfit-1);
48 Vclk=Vclk(1:tfit-1);
49 Iin_NAND=Iin_NAND(1:NSample);
50 Pin_NAND=Pin_NAND(1:NSample);
51 Vc=Vc(1:NSample);
52
53 Tp=td(tfit-1)+td(tfit-2);
54 d_1_LED=1./length(LEDposition).*100;
55 d_LEDS=LEDS./length(LEDposition).*100;
56 period = Tp.*10;
57
58 for j=1:length(td)
59     if Vclk(j)~=0
60         if counter<10
61             counter=counter+1;
62         else
63             counter=1;
64         end
65         [ILED(j/2),PLED(j/2),Pin_clkDIV(j/2)]=ClockDivider(counter,
```

```
                LEDposition,VOH_CLKDIV,Vf,RLED,Vcc);
    end
end

ILED_t=zeros(1,NSample);
PLED_t=zeros(1,NSample);
Pin_clkDIV_t=zeros(1,NSample);

TpSample=(round(Tp.*NSample./T));
for k=1:length(ILED)
    ILED_t((k-1)*TpSample+1:k*TpSample)=ILED(k).*ones(1,TpSample);
    PLED_t((k-1)*TpSample+1:k*TpSample)=PLED(k).*ones(1,TpSample);
    Pin_clkDIV_t((k-1)*TpSample+1:k*TpSample)=Pin_clkDIV(k).*ones(1,
        TpSample);
end

Iin_tot=Iin_NAND+ILED_t;
Pin_tot=Pin_NAND+Pin_clkDIV_t;
Pave = sum(Pin_tot)./length(Pin_tot);
PLEDave=sum(PLED_t)./length(PLED_t);
PinCLKDIVave=sum(Pin_clkDIV_t)./length(Pin_clkDIV_t);
PNANDave=sum(Pin_NAND)./length(Pin_NAND);
PLEDfrac=PLEDave./Pave;

endsample=zeros(1,length(Vclk));
endsample(1)=round(td(1).*NSample./T);
Vclk_t(1:endsample(1))=Vclk(1).*ones(1,endsample(1));
for L=2:length(Vclk)
    endsample(L)=endsample(L-1)+round(td(L).*NSample./T);
    Vclk_t(endsample(L-1)+1:endsample(L))=Vclk(L).*ones(1,endsample(L
        )-endsample(L-1));
end

Vclk_t=Vclk_t(1:NSample);

figure
subplot(2,2,3)
plot(t, ILED_t)
title('Current delivered to the LEDs')
xlabel('Time [s]')
ylabel('Current [A]')
set(gca,'fontsize',20);

subplot(2,2,1)
plot(t,Vc);
title('Voltage over the capacitor')
xlabel('Time [s]')
ylabel('Voltage [V]')
```

```
111 set(gca,'fontsize',20);
112
113 subplot(2,2,2)
114 plot(t,Iin_NAND);
115 title('Current drawn by the oscillator')
116 xlabel('Time [s]')
117 ylabel('Current [A]')
118 set(gca,'fontsize',20);
119
120 subplot(2,2,4)
121 plot(t,Iin_tot)
122 title('Source output current')
123 xlabel('Time [s]')
124 ylabel('Current [A]')
125 set(gca,'fontsize',20);
126
127 figure
128 subplot(2,2,1)
129 plot(t,Pin_NAND)
130 title('Power drawn by the oscillator')
131 xlabel('Time [s]')
132 ylabel('Power [W]')
133 set(gca,'fontsize',20);
134
135 subplot(2,2,2)
136 plot(t,Pin_clkDIV_t)
137 title('Power drawn by the IC, LEDs and resistor')
138 xlabel('Time [s]')
139 ylabel('Power [W]')
140 set(gca,'fontsize',20);
141
142 subplot(2,2,3)
143 plot(t,Pin_tot);
144 title('Power delivered by the source')
145 xlabel('Time [s]')
146 ylabel('Power [W]')
147 set(gca,'fontsize',20);
148
149 subplot(2,2,4)
150 plot(t, PLED_t)
151 title('Power delivered to the LEDs')
152 xlabel('Time [s]')
153 ylabel('Power [W]')
154 set(gca,'fontsize',20);
```

```
1 function [Vclk,td,Iin,Pin,Vc,newState]=NANDoscillator(State,R2,C1,VIH
      ,VIL,VOH,Vcm,Vcc,t)
2       if State==1
3           Vclk=0;
```

```
4           td=-R2.*C1.*log((VIH-VOH)./(Vcm-VOH));
5           V1I=VOH+(Vcm-VOH).*exp(-t./(R2.*C1));
6           Iin=(VOH-V1I)./R2;
7           Pin=Iin.*Vcc;
8           newState=2;
9           Vc=-V1I;
10      elseif State==2
11          Vclk=VOH;
12          td=-R2.*C1.*log(VIL./(VOH-Vcm));
13          V1I=(VOH-Vcm).*exp(-t./(R2.*C1));
14          Iin=V1I./R2;
15          Pin=Iin.*Vcc;
16          newState=1;
17          Vc=VOH-V1I;
18      end
19  end
```

```
1  function [ILED,PLED,Pin]=ClockDivider(counter,LEDinputs,VOH,Vf,RLED,
       Vcc)
2  if LEDinputs(counter)==1
3      ILED=(VOH-Vf)./RLED;
4      PLED=ILED.*Vf;
5      Pin=ILED.*Vcc;
6  else
7      ILED=0;
8      PLED=0;
9      Pin=0;
10 end
```

Bibliography

[1] W. K. Zhu, M. Zhu, C. Y. Yuan, and R. M. Diao, "Study on the improvement of microprism retroreflective material," in *Micro-Nano Technology XV*, ser. Key Engineering Materials, vol. 609. Trans Tech Publications, 6 2014, pp. 271–280.

[2] I. Kwan and J. Mapstone, "Visibility aids for pedestrians and cyclists: a systematic review of randomised controlled trials," *Accident Analysis & Prevention*, vol. 36, no. 3, pp. 305 – 312, 2004.

[3] "Million mile light," May 2019, https://www.batteryfree.co.uk/.

[4] A. CRAWFORD, "The perception of light signals: The effect of the number of irrelevant lights," *Ergonomics*, vol. 5, no. 3, pp. 417–428, 1962. [Online]. Available: https://doi.org/10.1080/00140136208930612

[5] R. Blake and M. Shiffrar, "Perception of human motion," *Annual Review of Psychology*, vol. 58, no. 1, pp. 47–73, 2007, pMID: 16903802. [Online]. Available: https://doi.org/10.1146/annurev.psych.57.102904.190152

[6] J. Kremers, R. C. Baraas, and N. J. Marshall, *Human color vision.* Springer, 2016, vol. 5.

[7] M. Eloholma, M. Viikari, L. Halonen, H. Walkey, T. Goodman, J. Alferdinck, A. Freiding, P. Bodrogi, and G. Várady, "Mesopic models-from brightness matching to visual performance in night-time driving: a review," *Lighting Research & Technology*, vol. 37, no. 2, pp. 155–173, 2005. [Online]. Available: https://doi.org/10.1191/1365782805li135oa

[8] J. Roufs, *Light as a true visual quantity : principles of measurement*, ser. CIE publication. Commission Internationale de l'Éclairage, 1978, the following members of TC 1.4 took part in the preparation of this Technical Report: W. Adrian, Canada; M. Aguilar, Spain ; E. Alnaes, Norway; F. Fankhauser, Switzerland; V. Gavriiski, Bulgaria; D. Gligo, Yugoslavia; M. Ikeda, Japan; A. Ionescu, Romania; J. John, Czechoslovakia; P. Kaiser, Canada; J. Kingsley, Australia; J. Kinney, USA; ; . Konarski, Poland; T. Krakau, Sweden; E. Krogh, Denmark; P. Lehtinen, Finland; E. Meyer, South Africa; D. Palmer, Great Britain; D. Parra, France; L. R. Ronchi, Italy; J. Roufs, The Netherlands; J. Schanda, Hungary; A. Tchetchik, Israel; G. Verriest, Belgium.

[9] Y. Ohno, "Physical measurement of flashing lights–now and then," in *Proc. CIE Expert Symposium on Temporal and Spatial Aspects of Light and Colour Perception and Measurements*, 2002. [Online]. Available: https://ws680.nist.gov/publication/get_pdf.cfm?pub_id=841704

[10] A. CRAWFORD, "The perception of light signals : The effect of mixing flashing and steady irrelevant lights," *Ergonomics*, vol. 6, no. 3, pp. 287–294, 1963. [Online]. Available: https://doi.org/10.1080/00140136308930708

[11] J. M. Wood, R. A. Tyrrell, R. Marszalek, P. Lacherez, and T. Carberry, "Bicyclists overestimate their own night-time conspicuity and underestimate the benefits of retroreflective markers on the moveable joints," *Accident Analysis & Prevention*, vol. 55,

pp. 48 – 53, 2013. [Online]. Available: http://www.sciencedirect.com/science/article/pii/S0001457513000821

[12] A. Mills, "Lighting: The progress & promise of leds," *III-Vs Review*, vol. 17, no. 4, pp. 39 – 41, 2004. [Online]. Available: http://www.sciencedirect.com/science/article/pii/S0961129004004661

[13] M. Fontoynont, "Led lighting, ultra-low-power lighting schemes for new lighting applications," *Comptes Rendus Physique*, vol. 19, no. 3, pp. 159 – 168, 2018, lEDs: The new revolution in lighting / Les LED : la nouvelle révolution de l'éclairage. [Online]. Available: http://www.sciencedirect.com/science/article/pii/S1631070517300944

[14] M. Maksimainen, M. Puolakka, E. Tetri, and L. Halonen, "Veiling luminance and visual adaptation field in mesopic photometry," *Lighting Research & Technology*, vol. 49, no. 6, pp. 743–762, 2017. [Online]. Available: https://doi.org/10.1177/1477153516637400

[15] S. Fotios and Q. Yao, "The association between correlated colour temperature and scotopic/photopic ratio," *Lighting Research & Technology*, vol. 0, no. 0, p. 1477153518779637, 0. [Online]. Available: https://doi.org/10.1177/1477153518779637

[16] Jägerbrand and A. K., "New framework of sustainable indicators for outdoor led (light emitting diodes) lighting and ssl (solid state lighting)," *Sustainability*, vol. 7, no. 1, pp. 1028–1063, 2015. [Online]. Available: http://www.mdpi.com/2071-1050/7/1/1028

[17] H. Jin, S. Jin, L. Chen, S. Cen, and K. Yuan, "Research on the lighting performance of led street lights with different color temperatures," *IEEE Photonics Journal*, vol. 7, no. 6, pp. 1–9, Dec 2015.

[18] I. Kwan and J. Mapstone, "Interventions for increasing pedestrian and cyclist visibility for the prevention of death and injuries," *Cochrane Database of Systematic Reviews*, no. 4, 2006. [Online]. Available: https://doi.org//10.1002/14651858.CD003438.pub2

[19] T. Khan, P. Bodrogi, and Q. Vinh, *LED Lighting : Technology and Perception.* John Wiley and Sons, incorporated, 2014.

[20] "Anec r&t study on requirements on lighting (light intensity) and reflectors of bicycles," June 2013.

[21] "Conrad electronic benelux b.v." June 2019, https://www.conrad.nl/.

[22] "Farnell," June 2019, https://nl.farnell.com/.

[23] "Rs components ltd," June 2019, https://nl.rs-online.com/web/.

[24] J. Moore, "Acrylonitrile-butadiene-styrene (abs) - a review," *Composites*, vol. 4, no. 3, pp. 118 – 130, 1973. [Online]. Available: http://www.sciencedirect.com/science/article/pii/0010436173905855

[25] J. J. Wolken, *Light Detectors, Photoreceptors, and Imaging Systems in Nature.* Oxford University Press, Incorporated, 1995.

[26] R. Marston, *Outline and pin designations (a) and basic functional diagram; (b) of the 4017B decade counter/divider IC.* Nuts and Volts. [Online]. Available: https://www.nutsvolts.com/uploads/wygwam/NV_0400_Marston_Figure01.jpg